AGU PUBLICATIONS

JGR

Journal of Geophysical Research: Earth Surface

RESEARCH ARTICLE
10.1002/2014JF003322

Key Points:
- High-resolution bathymetry delineates major active seafloor fault zones
- Transpression along steep faults produces basin inversion and basement uplift
- Active offshore fault systems may sustain long complex fault rupture

Supporting Information:
- Text S1, Figures S1, S2, and S4, and Tables S1–S4
- Figure S3

Correspondence to:
M. Legg,
mrlegg@verizon.net

Citation:
Legg, M. R., M. D. Kohler, N. Shintaku, and D. S. Weeraratne (2015), High-resolution mapping of two large-scale transpressional fault zones in the California Continental Borderland: Santa Cruz-Catalina Ridge and Ferrelo faults, *J. Geophys. Res. Earth Surf.*, *120*, 915–942, doi:10.1002/2014JF003322.

Received 29 AUG 2014
Accepted 21 APR 2015
Accepted article online 24 APR 2015
Published online 30 MAY 2015

High-resolution mapping of two large-scale transpressional fault zones in the California Continental Borderland: Santa Cruz-Catalina Ridge and Ferrelo faults

Mark R. Legg[1], Monica D. Kohler[2], Natsumi Shintaku[3], and Dayanthie S. Weeraratne[4]

[1]Legg Geophysical, Huntington Beach, California, USA, [2]Department of Mechanical and Civil Engineering, California Institute of Technology, Pasadena, California, USA, [3]Department of Geological Sciences, Brown University, Providence, Rhode Island, USA, [4]Department of Geological Sciences, California State University, Northridge, California, USA

Abstract New mapping of two active transpressional fault zones in the California Continental Borderland, the Santa Cruz-Catalina Ridge fault and the Ferrelo fault, was carried out to characterize their geometries, using over 4500 line-km of new multibeam bathymetry data collected in 2010 combined with existing data. Faults identified from seafloor morphology were verified in the subsurface using existing seismic reflection data including single-channel and multichannel seismic profiles compiled over the past three decades. The two fault systems are parallel and are capable of large lateral offsets and reverse slip during earthquakes. The geometry of the fault systems shows evidence of multiple segments that could experience throughgoing rupture over distances exceeding 100 km. Published earthquake hypocenters from regional seismicity studies further define the lateral and depth extent of the historic fault ruptures. Historical and recent focal mechanisms obtained from first-motion and moment tensor studies confirm regional strain partitioning dominated by right slip on major throughgoing faults with reverse-oblique mechanisms on adjacent structures. Transpression on west and northwest trending structures persists as far as 270 km south of the Transverse Ranges; extension persists in the southern Borderland. A logjam model describes the tectonic evolution of crustal blocks bounded by strike-slip and reverse faults which are restrained from northwest displacement by the Transverse Ranges and the southern San Andreas fault big bend. Because of their potential for dip-slip rupture, the faults may also be capable of generating local tsunamis that would impact Southern California coastlines, including populated regions in the Channel Islands.

1. Introduction

Large-scale active oblique-slip fault systems in submarine environments may produce large earthquakes with seafloor deformation that generates potentially destructive tsunamis (e.g., 12–13 April 2014, Solomon Islands, $M_w = 7.6$, 7.4; 22 August 1949, Queen Charlotte Islands, $M_s = 8.1$; and 28 October 2012, Haida Gwaii, $M_w = 7.7$). Because erosion is subdued in deep submarine environments, the morphology of the seafloor provides an excellent record of tectonic deformation that may be used to evaluate regional tectonic evolution and earthquake hazard potential. Basin-filling sedimentary sequences imaged in seismic reflection data provide additional information to constrain the three-dimensional structural geometry. The history of deformation can be discerned where geological ground truth is available from deep boreholes and shallow core or dredge samples on outcrops.

Offshore Southern California, part of the active Pacific-North America transform plate boundary (Figure 1), the seafloor is deformed by several large oblique-slip fault systems. Here high-resolution bathymetry data are available to map the seafloor morphology, numerous seismic reflection surveys exist to confirm subsurface structural interpretations, and widespread seafloor and subbottom samples [*Vedder*, 1990] provide information on timing of deformation. Our investigation of the seafloor morphology of two large-scale active transpressional fault systems in the California Continental Borderland presents evidence for the transpressional partitioning of strain between right slip and oblique slip on offshore fault systems. Our mapping of their continuity and geometry shows that transpression occurs on major, long, continuous right-slip faults and on numerous oblique-slip faults. Uplift of tectonic (crustal) blocks is accommodated by vertical displacement on and between high-angle faults, including vertical right-lateral faults within the entire Borderland.

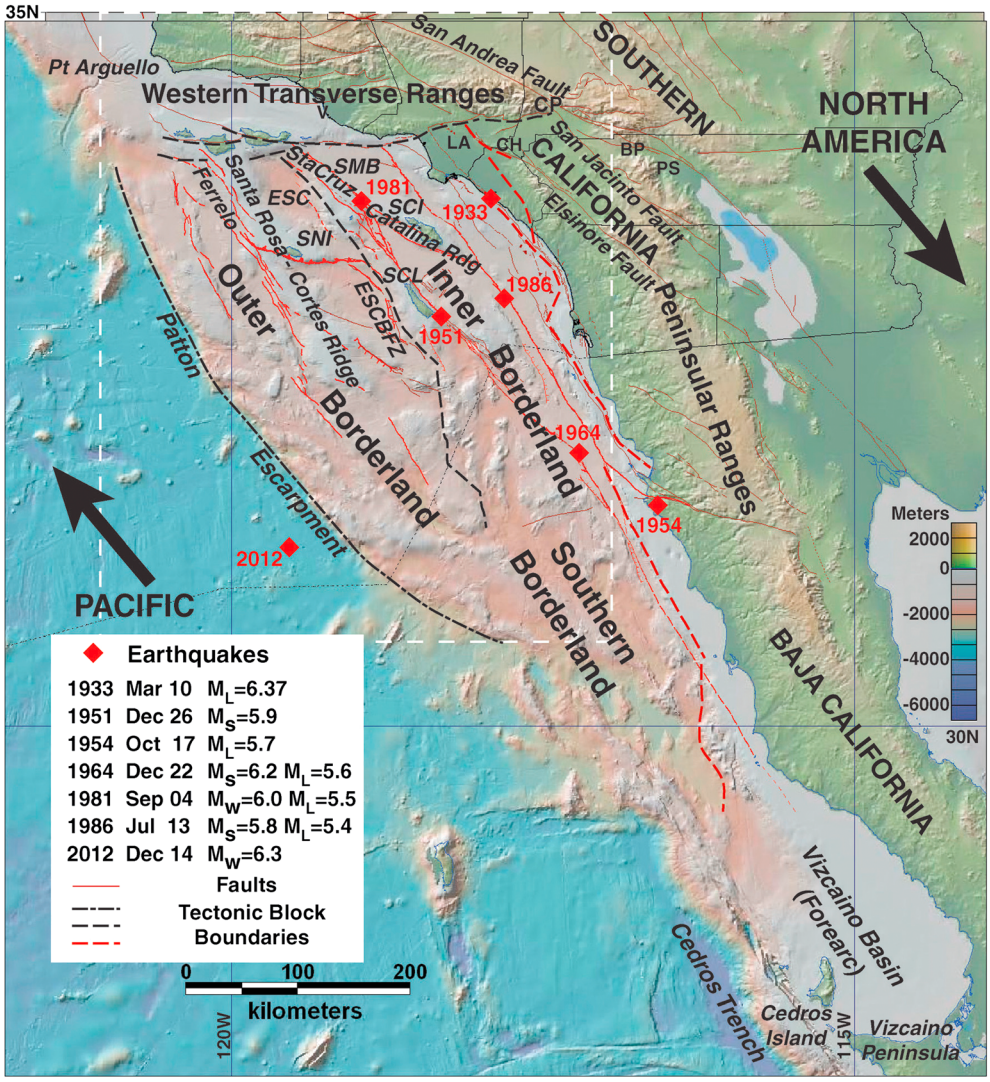

Figure 1. Map of the California Continental Borderland showing major tectonic features and moderate earthquake locations ($M > 5.5$). The dashed box shows area of this study. The large arrows show relative plate motions for the Pacific-North America transform fault boundary (~N40° ± 2°W; RM2 and PA-1 [*Plattner et al.*, 2007]). BP = Banning Pass, CH = Chino Hills, CP = Cajon Pass, LA = Los Angeles, PS = Palm Springs, V = Ventura, ESC = Santa Cruz Basin, ESCBZ = East Santa Cruz Basin fault zone, SCI = Santa Catalina Island, SCL = San Clemente Island, SMB = Santa Monica Basin, and SNI = San Nicolas Island. Base map from GeoMapApp/Global Multi-Resolution Topography (GMRT) [*Ryan et al.*, 2009].

Large crustal earthquakes ($M > 7$) often involve long ruptures of complex fault systems, e.g., 1906 San Francisco, 1976 El Asnam, 1992 Landers, 1999 Chi-Chi, 1999 Izmit, 2002 Denali, 2008 Wenchuan, 2010 El Major-Cucapah, and 2012 offshore Sumatra. Consequently, detailed mapping of faulting and deformation patterns is required to estimate the likelihood of multisegment and multifault ruptures on long fault zones. In addition, seismicity data provide information on the deep fault character and possible fault interactions and strain partitioning in the oblique-fault system.

Large offshore transpressional fault systems such as the Queen Charlotte Islands (offshore British Columbia), New Zealand and the Macquarie Ridge, the Caribbean, and the Scotia plate perimeter in the southwest Atlantic Ocean may exhibit similar character to the California Continental Borderland fault systems examined in this study. Large earthquakes affect these submarine plate boundaries [*James et al.*, 2013; *Dolan and Mann*, 1998; *Bohoyo et al.*, 2007], and oblique slip often generates local tsunamis [*Lay et al.*, 2013]. Through our mapping, we find that offshore Southern California faults are also long and continuous and may be capable of experiencing a significant amount of oblique slip over long-distance rupture.

This study focuses on two of the largest Borderland fault zones, the Santa Cruz-Catalina Ridge and the Ferrelo (Figure 1), where we obtained new bathymetry data to compare the character and recency of faulting. Displacement on these fault zones accommodates the tectonic movement of crustal blocks within the western half of the Pacific-North America transform plate boundary in Southern California. Here active deformation appears to reach as far west as the deepwater Pacific oceanic crust based on the 14 December 2012 M_w6.3 earthquake located more than 260 km west of Baja California [*Hauksson et al*., 2013]. Based on this comprehensive mapping effort combining new with existing data, we propose a "logjam" model for offshore deformation: obstruction to northwest directed right-lateral strike slip imposed by the western Transverse Ranges shifts north directed shortening southward as far as San Nicolas Island, through a crustal block consisting of the northern Santa Rosa-Cortes Ridge, which is stuck like a log at a dam in a river. Thus, moderate-to-low-angle reverse (thrust) faulting may occur hundreds of kilometers away from the western Transverse Ranges due to this logjam effect.

2. Location and Tectonic Background

The California Continental Borderland (Figure 1) represents the continental margin located offshore Southern California, USA, and northern Baja California, Mexico [*Shepard and Emery*, 1941; *Emery*, 1960; *Moore*, 1969]. The Borderland is 100–250 km wide and consists of a complex series of ridges and troughs that lie subparallel to the coast separating the land from the deep Pacific Ocean basin. The Borderland extends from Point Arguello in the north to the Vizcaino Peninsula and Cedros Island in the south (Figure 1). It is separated from the deep Pacific Ocean basin on the west by the Patton Escarpment and the Cedros Trench within its southern section. Although its eastern boundary is considered to be the shoreline, Borderland physiography extends onshore in places including the Los Angeles, Ventura, and Vizcaíno Basins [*Shepard and Emery*, 1941; *Moore*, 1969; *Vedder et al*., 1974]. This study focuses on the section of the Northern Borderland where northwest trending structures are dominant and may be influenced by convergence with the western Transverse Ranges.

Mesozoic through early Tertiary history of the Southern California region (Figure 2) was dominated by subduction of the Farallon plate beneath the North America continental margin [*Atwater*, 1970]. The remnants of the former subduction zone are recognized as tectonostratigraphic terranes within the Borderland [*Howell and Vedder*, 1981]. The Outer Borderland comprises the accretionary wedge and fore-arc blocks that once existed along the coast north of Vizcaino Basin, whereas the Inner Borderland comprises the rift that was left behind [*Legg*, 1991; *Crouch and Suppe*, 1993] as the western Transverse Ranges fore-arc block separated and rotated about a vertical axis away from the Southern California margin (Figure 1) [*Kamerling and Luyendyk*, 1979, 1985]. Major fault systems initially inferred to be subvertical strike-slip shear zones [*Junger*, 1976; *Legg and Kennedy*, 1979; *Vedder*, 1987] separate these crustal blocks. Low-angle faults (décollements) may define some block boundaries [*Nicholson et al*., 1994]. Inherited structural fabric and rheology from Mesozoic to early Tertiary subduction are inferred to have a significant impact on subsequent deformation and fault evolution [*Legg*, 1991; *Legg et al*., 2007; *Sorlien et al*., 2013] (Figure 2).

The California Continental Borderland physiography developed during the Miocene evolution of the transform plate boundary [*Atwater*, 1970; *Vedder et al*., 1974]. As the transform fault boundary lengthened southward, migration of the East Pacific Rise spreading center offshore Southern California heated and weakened the adjacent continental crust. Northwest movement of the Pacific plate away from the California margin [*Atwater and Stock*, 1988] created oblique extension (transtension) along an irregular plate boundary [*Lonsdale*, 1991; *Nicholson et al*., 1994]. Oblique rifting of the continental margin was largely responsible for the basin-and-ridge physiography of the Borderland [*Legg*, 1991; *Crouch and Suppe*, 1993]. Widespread northwest trending oblique- and right-slip faulting above a regional low-angle normal fault (detachment) system exhumed former deeply subducted oceanic crust of the ancient Farallon plate [*Legg*, 1991; *Crouch and Suppe*, 1993; *Bohannon and Geist*, 1998]. Crustal thinning by extreme extension of the former accretionary wedge created intense volcanic activity during the middle Miocene epoch [*Weigand*, 1994; *Luyendyk et al*., 1998] when faulting broke through the detachment possibly due to formation of a slab window/gap in the former subduction megathrust [*Wilson et al*., 2005]. An archipelago of large calderas formed along the axis of the Inner Borderland Rift [*Legg et al*., 2004]. The circular

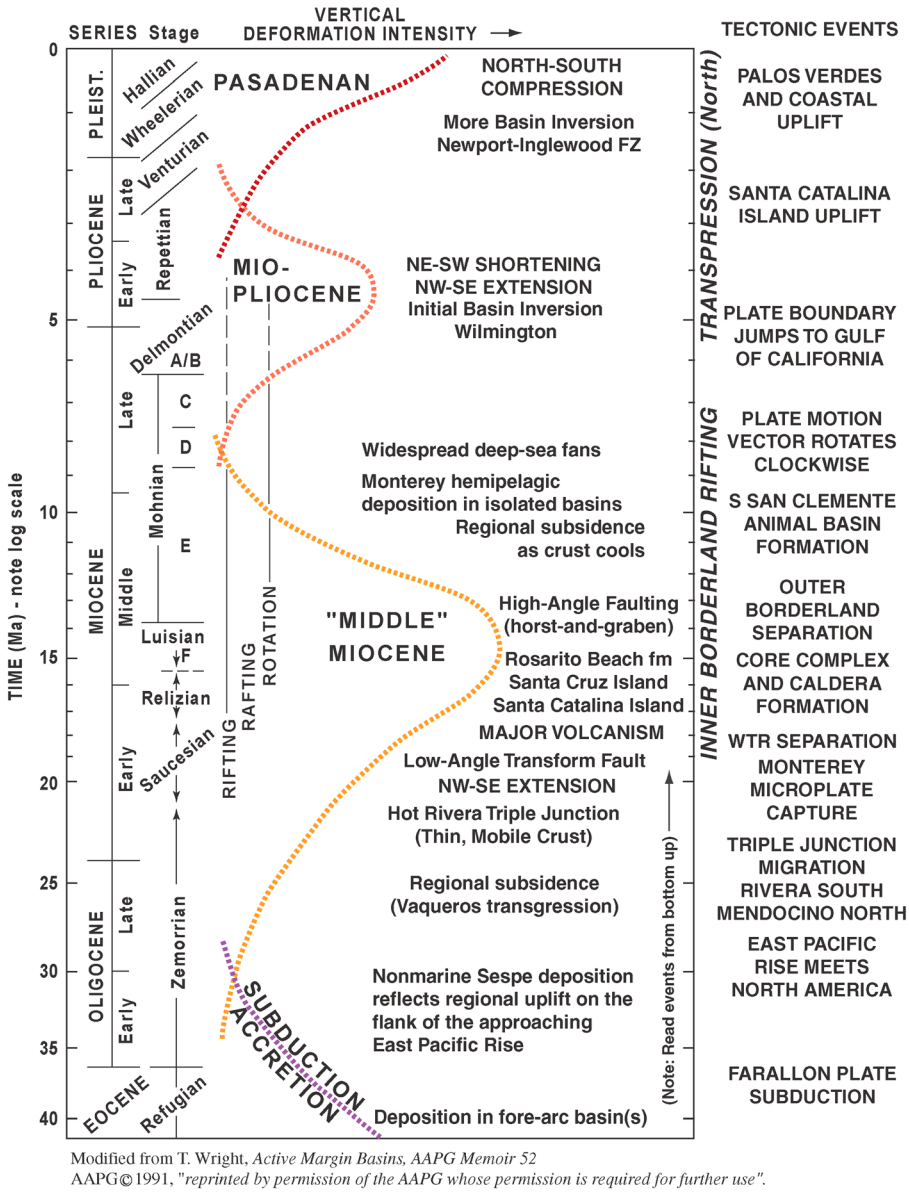

Figure 2. Chronology of major Cenozoic events in the Southern California region (after *Wright* [1991] and *Legg and Kamerling* [2012]). Intensity of tectonic deformation is represented by the curve. Local (Los Angeles Basin) biostratigraphic zonation is shown. The slanted labels for Neogene stages represent the time-transgressive nature of these boundaries.

morphology of these calderas provides piercing points to estimate long-term right-lateral slip on major Inner Borderland faults (e.g., Emery Knoll and offset crater rim [*Legg et al*., 2004]).

Late Miocene cooling of the rifted Borderland led to subsidence of most Borderland basins [*Vedder et al*., 1979; *Vedder*, 1987; *Sorlien et al*., 2013] and is manifested in the terraces and smooth eroded surfaces of many Borderland ridges that lie far below subsequent sea level lowstands. Pliocene to Recent transpression due to a clockwise rotation in the relative plate motion vector [*Atwater and Stock*, 1988] and the eastward jump in the transform plate boundary resulted in basin inversion along Miocene transtensional faults [*Wright*, 1991; *Legg et al*., 2007; *Legg and Kamerling*, 2012; *Sorlien et al*., 2013]; former extensional faults reversed direction and uplifted overlying basin sediments [cf. *Buchanan and Buchanan*, 1995]. Abundant folding and reverse focal mechanisms of earthquakes demonstrate convergence at the Transverse Ranges but also northeast directed shortening within the Inner Borderland [*Hauksson and Jones*, 1988; *Fisher et al*., 2009].

Recognizing that Pliocene to Recent transpression followed Miocene oblique rifting in the Borderland is the basis for understanding the active transpression examined in this study. More accurate timing of the transition from oblique extension to convergence is derived from the seismic profiles where stratigraphic control from seafloor and subsurface samples are available [e.g., *Sorlien et al*., 2013]. A gradient in the degree of shortening was recognized by *Legg* [1985] in the Inner Borderland where shortening diminished southward with extension persisting offshore northern Baja California.

3. Methods and Data

We use geomorphology to map active faults based on identification of features associated with recent upper crustal deformation [cf. *Slemmons*, 1973; *Yeats et al*., 1997]. *Legg et al*. [1989] described the morphology observed along active submarine strike-slip faults offshore Southern California. Elevated areas along ridges preserve more ancient deformation features than adjoining basin areas. While slope failures may bury or obscure active fault structures, they also record fault activity and display subsequent fault displacements. We use stratigraphy defined by high-resolution seismic reflection profiles combined with seafloor and subbottom samples to constrain the timing of the deformation.

3.1. Multibeam Bathymetry Data

Large gaps remain in high-resolution bathymetric maps of the Northern Borderland (Figure 3). The 2010 ALBACORE (Asthenospheric and Lithospheric Broadband Architecture from the California Offshore Region Experiment) cruise gathered 4593 line-km of new data intentionally designed to fill in some of the gaps, particularly along major escarpments where evidence of active faulting may exist [*Kohler and The Science Party*, 2010] (Figure 3). Updated maps of high-resolution bathymetry were prepared for this study using the new data [*Shintaku et al*., 2010] combined with existing (prior to 2010) multibeam bathymetry data from 126 previous research cruises available from the National Geophysical Data Center (NGDC).

The combined bathymetry data sets were gridded at 100 m spacing to produce map images for four areas presented here (Figure 3). The first area (North Borderland) provides regional coverage including most of the Northern Borderland from the western Transverse Ranges beyond Point Arguello to the southern San Diego Trough offshore Baja California. The second area (Catalina) covers the northern part of the Inner Borderland and eastern Outer Borderland from San Nicolas Island to Oceanside centered near Catalina Basin and Santa Catalina Island. The third area (North Ferrelo) covers the northern Outer Borderland, from the North Channel Islands south to beyond the San Nicolas Island escarpment. The fourth area (South Ferrelo) covers the central Outer Borderland from San Nicolas Island to Velero Basin west of northern Baja California. Images were produced at eight different Sun angles (45°, 90°, 135°, 180°, 225°, 270°, 315°, and 360°) to highlight different aspects of seafloor morphology enhanced by shadows or bright reflections from bathymetric relief. The map images were georegistered into the MapInfo™ Geographic Information System for interpretation and mapping of faults and other seafloor features (Table S1 in the supporting information).

3.2. Seismic Data

In addition to high-resolution bathymetry, we used selected profiles from existing Borderland seismic reflection data to carry out subsurface verification of faults identified from the seafloor morphology (Figure S1 in the supporting information). We used extensive, deep-penetration multichannel seismic (MCS) reflection data, including U.S. Geological Survey (USGS) and exploration industry profiles available from the National Archive of Marine Seismic Surveys [*National Archive of Marine Seismic Surveys* (*NAMSS*), 2006], to interpret deeper crustal structure and to confirm fault character. Other investigations provide more detailed subsurface mapping based on the seismic reflection data in the region [e.g., *Junger*, 1979; *Crouch*, 1981; *Vedder et al*., 1986; *Chaytor et al*., 2008; *Schindler*, 2010; *De Hoogh*, 2012], which we used to correlate with our geomorphic interpretations. We also used historical seismicity data including published earthquake hypocenter locations and focal mechanisms from regional seismicity investigations (Table S2 in the supporting information) [*Astiz and Shearer*, 2000; *Hauksson*, 2011; *Hauksson et al*., 2012; *Yang et al*., 2012] to compare to the fault mapping results presented here. This was to define fault character, segmentation, and tectonic deformation more accurately to seismogenic depths.

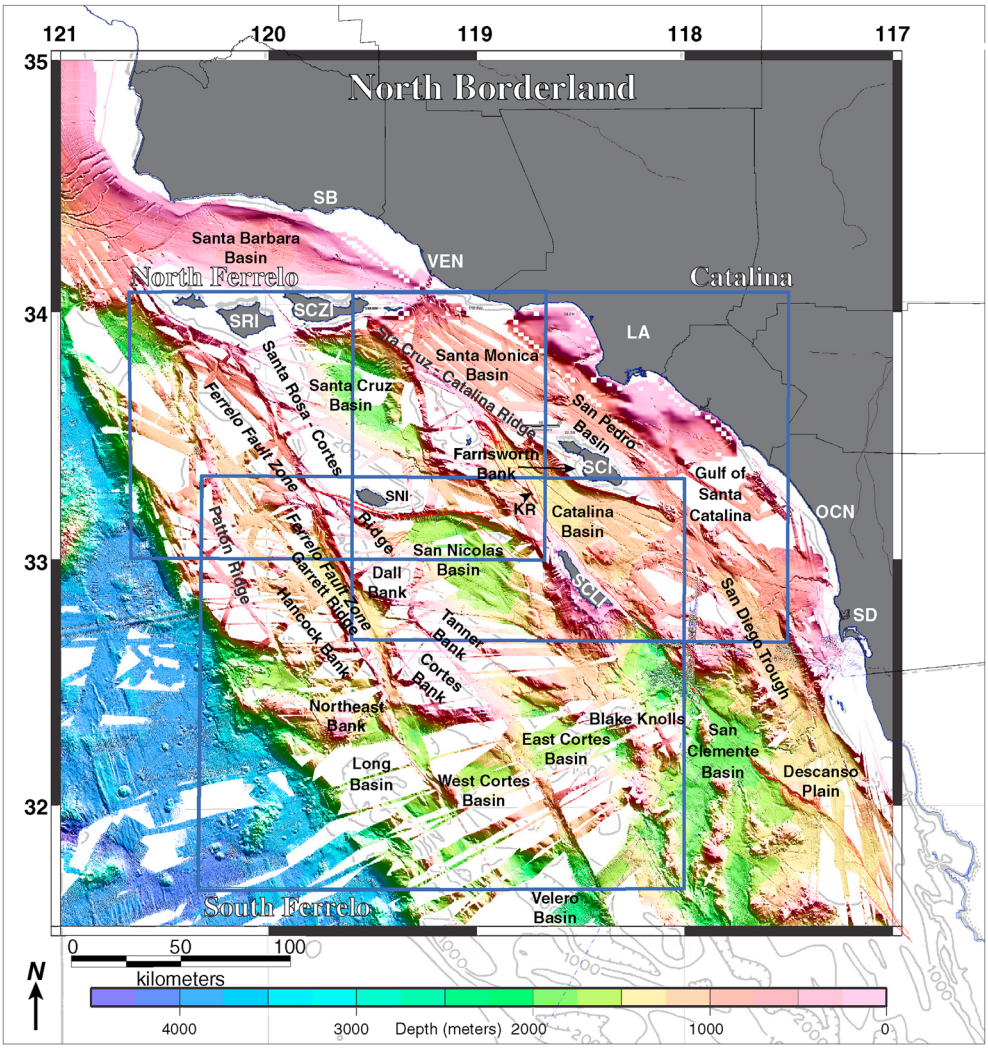

Figure 3. Map showing the North Borderland multibeam bathymetry coverage used in this study. "North Borderland" refers to entire region. The blue boxes outline three regions: "Catalina," "North Ferrelo," and "South Ferrelo" for focused active fault investigations using multibeam bathymetry (Table S1 in the supporting information). KR = Kimki Ridge, SRI = Santa Rosa Island, SCZI = Santa Cruz Island, SCI = Santa Catalina Island, SCLI = San Clemente Island, SB = Santa Barbara, VEN = Ventura, LA = Los Angeles, OCN = Oceanside, and SD = San Diego.

High-resolution MCS and single-channel data from the USGS [*National Archive of Marine Seismic Surveys* (*NAMSS*), 2006; *InfoBank*, 2013], from academic research cruises archived in the NGDC, and from data compiled by Legg over the past three decades [e.g., *Legg*, 1985; *Legg et al*., 2007] are used here to confirm shallow fault character and recency of activity. In many areas, shallow basement (acoustic basement that obscures deeper seismic imaging) makes it difficult to identify faults with confidence; the high-resolution bathymetry enables increased confidence in identification of faults that deform the seafloor. We also used offsets observed in Quaternary deposits locally in small basins along the fault strike or abundant seismicity to confirm fault activity in areas of uplifted acoustic basement.

We find that the shallow, high-resolution, seismic images are sufficient to demonstrate late Quaternary and Holocene displacement in basin sediments along the fault zones. We show selected deep penetration profiles, used to confirm deep structural character including fault dip and stratigraphic offsets. Coverage is more complete over the Santa Cruz-Catalina Ridge, whereas the Santa Rosa-Cortes Ridge has large gaps in coverage, especially in the central areas near San Nicolas Island and Cortes Bank (Figure S1 in the supporting information). The seafloor morphology is especially important for mapping potentially active fault traces in these areas.

4. Fault Descriptions

This study focuses on the following structures specifically because of their regional scale, active seismicity, large uncertainties regarding the fault geometries, the seismic potential of gaps between known segments, landslide history, and tsunamigenic potential. We used our newly compiled North Borderland map (Figure 3) to identify, map, and describe two major transpressional fault zones—the Santa Cruz-Catalina Ridge fault zone along the Santa Cruz-Catalina Ridge and the Ferrelo fault zone along the Santa Rosa-Cortes Ridge (Figures 1 and 3). Each focus area involved investigation of one or more major active tectonic structures in the Borderland that has contributed to large-scale deformation and tectonic evolution since the Miocene initiation of Pacific-North America plate interaction.

In the following discussion, we will refer to "fault systems" which represent a large collection of "fault zones" that are connected by geometry and tectonic history. Fault zones are collections of individual fault segments that are closely related along relatively narrow areas with significant lateral extent (>10 km for this regional study). Note that the Ferrelo fault system includes both the Ferrelo fault zone and the San Nicolas fault zone in our hierarchy. Fault segments include narrow and well-defined fault traces that are continuous and, in general, terminate at significant step overs or gaps in the fault zone. The "principal displacement zone" consists of the collection of fault traces and active structures that are interpreted to accommodate most of the tectonic slip [*Tchalenko*, 1970; *Biddle and Christie-Blick*, 1985].

4.1. Santa Cruz-Catalina Ridge Fault Zone

We mapped the Santa Cruz-Catalina Ridge fault zone, a major component of the laterally extensive (>600 km) San Clemente fault system that deforms the western half of the Inner Borderland and extends from the western Transverse Ranges to the Southern Borderland (Figures 1 and 4). The San Clemente fault system accommodates a significant proportion of right-lateral slip within the Inner Borderland Rift [*Legg and Goldfinger*, 2002] with several moderate earthquakes striking during the past century (Figures 1 and 4 and Table S2 in the supporting information). The Santa Cruz-Catalina Ridge is the major geomorphic feature associated with the northern section of the San Clemente fault system (Figures 1, 3, and 4). In general, the Santa Cruz-Catalina Ridge is composed of Miocene sedimentary and volcanic rocks overlying Mesozoic metamorphic basement rocks and Miocene intrusive rocks (Figure 5 and Figure S2 in the supporting information) [*Vedder et al*., 1974, 1986; *Junger and Wagner*, 1977]. The Santa Cruz-Catalina Ridge extends from Santa Cruz Island to the southeast about 25 km beyond the end of Santa Catalina Island (Figure 4) [*Vedder and Toth*, 1976]. Although Santa Barbara Island and Osborn Bank (Figure 4) are now adjacent to the Santa Cruz-Catalina Ridge, these features are considered to be on the northwest extension of the San Clemente Ridge [*Vedder and Toth*, 1976]. When combined with the Catalina fault to its intersection with the San Diego Trough fault, the Santa Cruz-Catalina Ridge fault zone length is about 170 km (Table S3 in the supporting information). For tsunami hazard estimation, *Legg et al.* [2004] modeled a large (140 km) transpressional fault rupture that extended from the Catalina Ridge to the Catalina fault and beyond along the San Diego Trough fault to the vicinity of Crespi Knoll (Figure 4).

4.1.1. Santa Catalina Island Section

Santa Catalina Island at the southern end of the Santa Cruz-Catalina Ridge fault zone forms a large rhomboid about 100 km long × 25 km wide and occupies the southern section of the ridge (Figure 4). Whereas most of the subaerial part of Santa Catalina Island consists of Mesozoic metamorphic rocks (Catalina Schist), the southeast part of the island is the core of a large Miocene volcano [*Vedder et al*., 1979]. Although no well-defined uplifted marine terraces have been confirmed subaerially [*Davis*, 2004], multiple submerged terraces surround Santa Catalina Island at depths ranging from 34 m to almost 350 m below sea level [*Emery*, 1958; *Francis and Legg*, 2010; *Castillo et al*., 2012]. Two major fault segments exist along escarpments on the southeast flank of the island: the Catalina fault and the Catalina Ridge fault (Figure 4). These escarpments form a right stepping echelon pattern with a step over distance of about 10 km. Canyons on the island are deflected in a dextral sense and are aligned with the Catalina Ridge escarpment for about 10 km; including the segment across the offshore shelf, fault overlap may reach a total of 20 km. The triangular region between the East San Clemente and Catalina Ridge faults has shape and dimensions that could fit into the step over area northwest of Farnsworth Bank (Figure 4) (C. Goldfinger, personal communications, 2001). As much as 50 km of right slip has been proposed along the Catalina Ridge fault

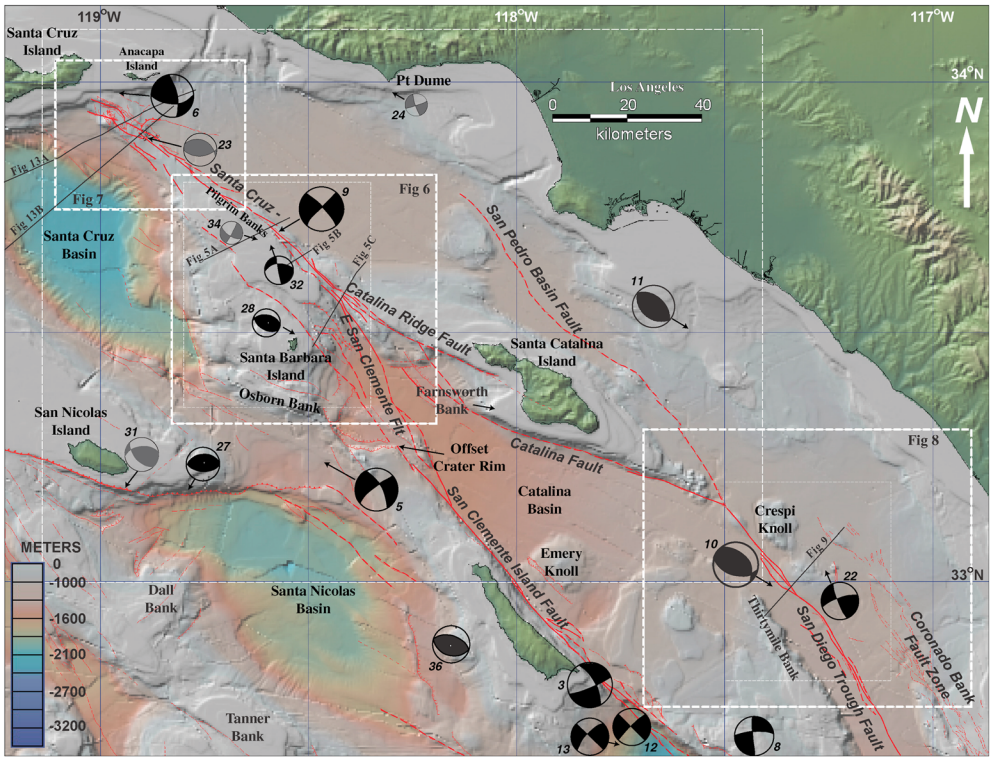

Figure 4. Map showing the Santa Cruz-Catalina Ridge and adjacent areas. The white dashed rectangles show locations of figures in the text. Focal mechanisms of significant earthquakes in the vicinity are shown with event numbers labeled (Table S2 in the supporting information). Strain partitioning is inferred based on the combination of strike-slip and thrust/reverse mechanisms along this transpressional fault zone. The black symbols denote well-constrained mechanisms (A-quality moment tensor solutions and historical first-motion solutions). The gray symbols denote less well-constrained mechanisms (B-quality moment tensor solutions). Data are from Southern California Earthquake Data Center (moment tensor catalog), *Legg* [1980], *Corbett* [1984], and *Hauksson and Jones* [1988]. The red lines are faults mapped for this study. The solid lines indicate faults with well-defined seafloor expression. The dashed faults indicate those that are more subtle in seafloor expression or are buried but are identified in seismic profiles. Basemap from GeoMapApp/GMRT [*Ryan et al.*, 2009].

section [*Chaytor et al.*, 2008]. Seismic profiles are interpreted to show southwest dipping faults along the Catalina escarpment [*ten Brink et al.*, 2000] with low-angle (~23°) to very steep (~80°) dips.

Our newly compiled multibeam-based bathymetry maps reveal a northeast facing (possibly normal separation) scarp along a 7 km ridge located about 2.8 km northwest of the projected Catalina fault trace (Figure 6a). About 2 km northeast of the scarp is a large 1.6 km square block located on the lower slope of the Catalina Ridge escarpment adjacent to the projected Catalina fault. A 5 km long × 1.6 km wide × 30 m deep trench, apparently cut when the block slid down the escarpment, exists to the northeast of the block [*Legg and Francis*, 2011]. Subtle slope inflections form a northwest trending lineament about 2 km upslope from the slide block; these are interpreted as evidence of another youthful fault trace that offsets the slide trench with uplift to the southwest to form another subtle upslope-facing scarp. At present, we have no sediment samples in this area to determine the age of either slide block or faulting, but their proximity and cross-cutting geometry may indicate earthquake triggering of slope failure. The apparent contradiction in fault dips with both normal and reverse separations in this area of uplift is consistent with strike-slip faulting in a transpressional zone and described as "flower" or "palm tree" structure in cross sections [*Wilcox et al.*, 1973; *Harding*, 1985; *Sylvester and Smith*, 1976; *Sylvester*, 1988].

To the north of Santa Catalina Island, the ridge bifurcates with Catalina Ridge on the east and Santa Barbara Island to the southwest (Figures 4 and 5a). The San Clemente fault zone merges with the Catalina Ridge fault zone along a submarine canyon in this area. Well-defined sedimentary sequences (possibly turbidites) inferred to be Monterey shale or equivalents [*Junger and Wagner*, 1977] appear to be squeezed vertically upward between upward diverging faults resembling a flower structure (Figure 5c; Oregon State University

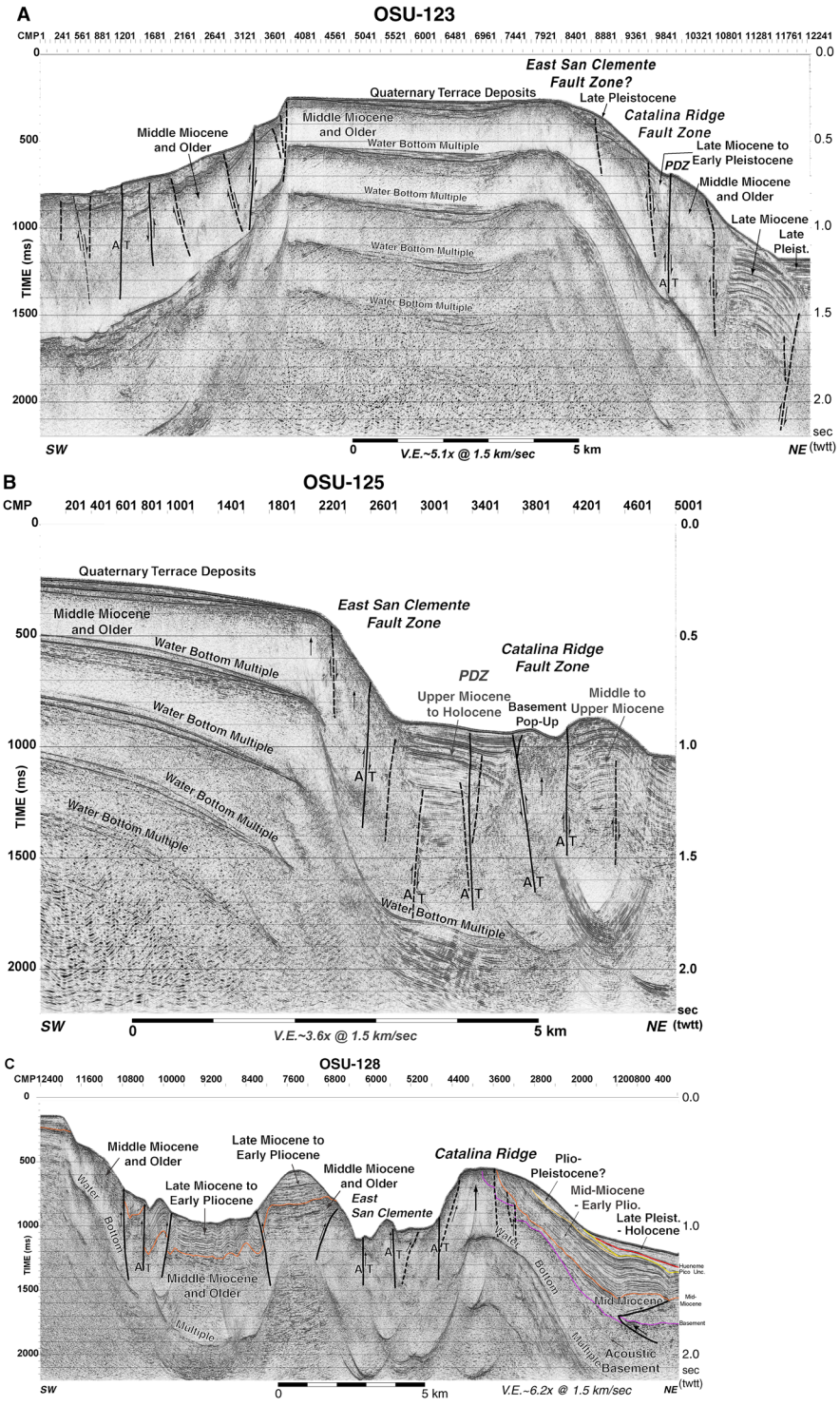

Figure 5. High-resolution 24-channel 4 kJ sparker seismic profiles along the Santa Cruz-Catalina Ridge (C. Goldfinger, personal communications, 2001). The profiles are arranged from north to south along the southern part of the ridge (see Figure 6a for profile locations). (a) Profile OSU-123 located north of Pilgrim Banks. The principal displacement zone for active right slip forms a narrow hillside valley on the northeast flank of the ridge. Steep faults on the west flank with normal separation (oblique?) are reactivated as the ridge was uplifted due to post-Miocene transpression. (b) Profile OSU-125 located across the epicentral region of the 4 September 1981 M_W6.0 earthquake. The main shock epicenter [*Corbett*, 1984] was located near the middle of the broad hillside valley (Linear Valley in Figure 6a) about halfway between profiles OSU-123 and OSU-125. (c) Profile OSU-128 located near the bifurcation of the Santa Cruz-Catalina Ridge east of Santa Barbara Island. The colored horizons are correlated to stratigraphy mapped by *Sorlien et al.* [2013] (see Figure 6 for profile location). The East San Clemente fault zone merges with the Catalina Ridge fault zone within the eastern valley (Figure 5a). Reverse slip is evident on several steep faults that bound blocks of sedimentary rocks that were squeezed up in this transpressional fault system.

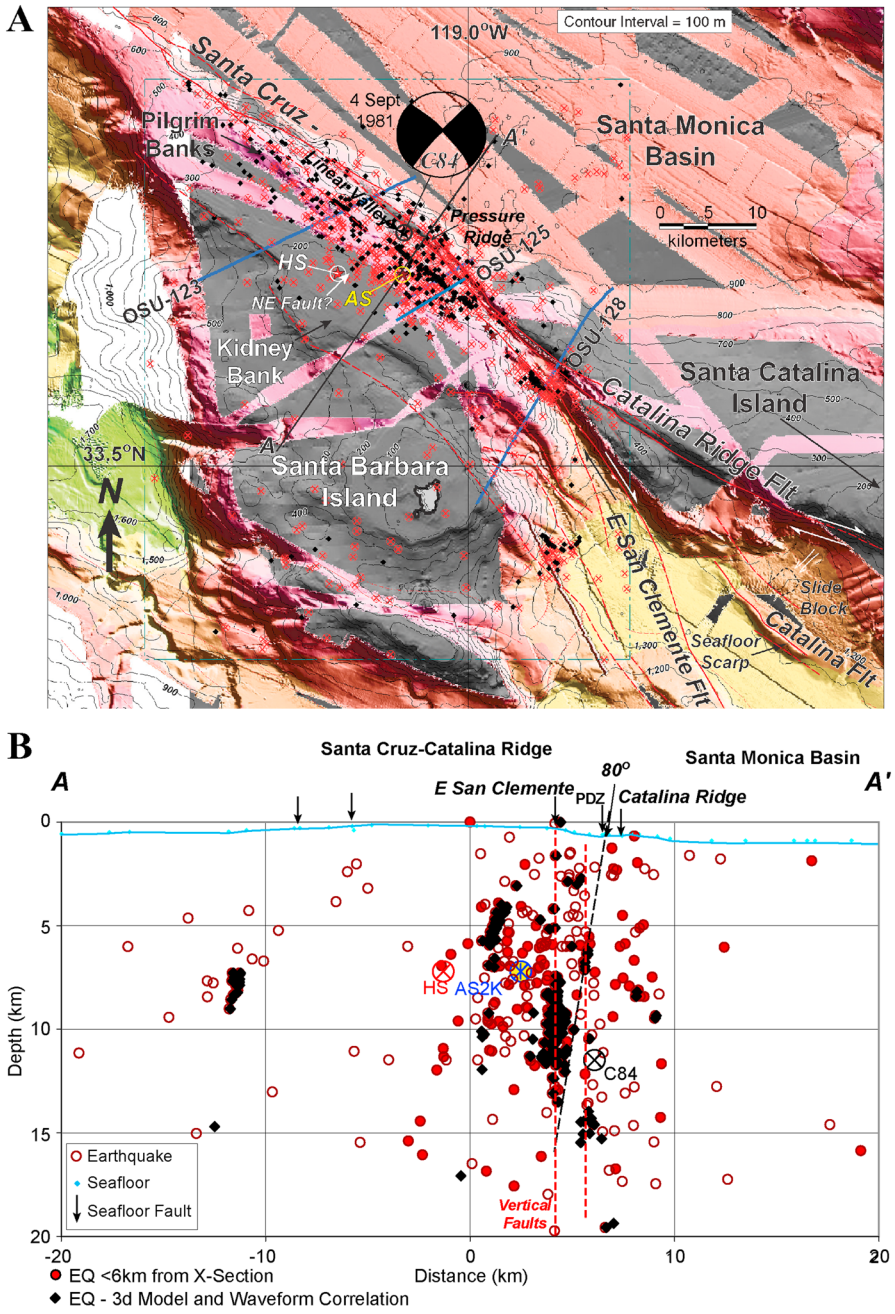

Figure 6. (a) Map showing location of the 4 September 1981 M_w6.0 Santa Barbara Island earthquake and aftershock relocations for events inside the dashed rectangle (red crosses) [*Hauksson et al.*, 2012]. The black diamonds are preferred locations based on both waveform correlations and a 3-D velocity model. Focal mechanism is from *Corbett* [1984]. The stars are locations of the main shock and larger aftershocks ($M_L > 3.8$) from various sources (HS = *Hauksson et al.* [2012], AS = *Astiz and Shearer* [2000], and C84 = *Corbett* [1984]). Large slide block with mile-wide trench is evident in the swath bathymetry on the escarpment at the northwest end of Santa Catalina Island. OSU seismic profiles are shown in Figure 5. Ridge with northeast facing scarp is located about 2 km southwest of the slide block and possibly aligned with traces of the Catalina fault at the base of the escarpment. Sun angle for swath bathymetry is from the northeast. (b) Seismicity cross-section A-A′ across the Santa Cruz-Catalina Ridge fault zone in the epicentral region of the 4 September 1981 earthquake. The black diamonds are preferred locations from *Hauksson et al.* [2012]. The open circles are 3-D model hypocenters with filled red dots showing hypocenters located within 6 km of the profile. The circled crosses with labels are hypocenters of the main shock from the various sources as in Figure 6a. The blue line shows seafloor elevation along profile. The arrows denote locations of fault traces mapped in this study; PDZ shows the principal displacement zone interpreted from seismic reflection profiles (Figure 5) and bathymetry data. The dashed lines show possible subsurface fault interpretations based on seismicity lineaments.

(OSU)-128) near the confluence of the East San Clemente and Catalina Ridge fault zones. With numerous northwest trending seafloor scarps, faulting is complex across a zone 10–20 km wide at this junction.

4.1.2. Pilgrim Banks Section

Along the ridge around Pilgrim Banks in the middle section of the Santa Cruz-Catalina Ridge, there is a broad area of relatively uniform depth, about 200–300 m below sea level (Figures 4 and 5a). In this area, *Chaytor et al.* [2008] identified multiple levels of submerged marine terraces which have similar elevations to those around Santa Catalina Island [*Castillo et al.*, 2012]. Along the eastern flank of the ridge between Pilgrim Banks and Kidney Bank (Figure 6a), uplift and tilting of layered sedimentary and volcaniclastic(?) sequences are juxtaposed against bedrock (Catalina Schist basement or Miocene volcanic rocks; Figure 5). Here steep to subvertical faults that form linear pressure ridges or pop-ups define the principal displacement zone of the Santa Cruz-Catalina Ridge fault zone. Both the San Clemente and the Catalina Ridge fault segments remain distinct and do not intersect for 20 km along the hillside valley. Layered sediments within a 30 km long hillside valley are offset by steep southwest dipping fault traces with several meters of vertical separation (Figure 5b; OSU-125). The hillside valley merges into the submarine canyon along the East San Clemente fault zone with a narrow branch continuing through a linear trench along the southwest flank of Catalina Ridge (Figures 4 and 5a).

To the north of Pilgrim Banks, the hillside valley narrows and becomes a small tectonic bench along the east flank of the Santa Cruz-Catalina Ridge (Figures 4 and 5a). Late Quaternary turbidites within the Santa Monica Basin to the east [*Normark et al.*, 2004] lap onto the older uplifted sequences. Acoustically transparent (hemipelagic) sequences near the seafloor on the slope appear continuous with subhorizontal layers in the basin fill. Seismic reflection profiles show subvertical faults for the principal displacement zone of the Santa Cruz-Catalina Ridge and San Clemente fault zones, and steep reverse-separation faults in the adjacent area (Figure 5), providing further evidence of the transpressional environment.

4.1.3. Northern Section

The northern section of the Santa Cruz-Catalina Ridge is about 10–20 km wide, and the ridge crest deepens from $<$100 m at Pilgrim Banks to $>$700 m midway between Pilgrim Banks and Santa Cruz Island. The principal displacement zone of the Santa Cruz-Catalina Ridge fault zone exists along the northeast flank of the ridge northwest of Pilgrim Banks (Figures 4 and 5). We use a dense grid of seismic profiles to map the principal fault traces where multibeam bathymetry is absent (Figure 7 and Figure S3 in the supporting information). Seismicity data show a zone of steep faulting extending 16 km or deeper into the crust (Figure 6b) [*Hauksson et al.*, 2012].

Near its intersection with Santa Cruz and Anacapa Islands, the ridge broadens and its crest rises to about 200 m below sea level (Figure 7). Numerous northwest trending seafloor lineaments define a broad fault zone with the principal displacement zone interpreted along the midnortheast side of the ridge. A gentle, right stepping "Lazy Z" fault bend exists in this area of complex deformation. A prominent N80°W lineament is inferred to be a branch fault that bounds a small block uplifted on the west side of the step over basin. The fault zone intersects the Santa Cruz Island fault in an embayment or offset of the west trending edge of the submarine terrace southeast of Santa Cruz Island (Figures 4 and 7) [*Chaytor et al.*, 2008].

Other more west trending faults adjacent to the Santa Cruz-Catalina Ridge appear to be thrust or reverse (oblique) faults associated with termination of northwest trending strike slip at the southern boundary of the western Transverse Ranges. Stratified Miocene basin sediments (Monterey Formation [*Junger*, 1979]) are tilted up on the northeast flank of the ridge (Figure 7 and Figure S3 in the supporting information; OSU-106). Poorly stratified, chaotic or nonreflective rocks including Miocene volcaniclastics (Blanca Formation) and Catalina Schist basement are uplifted and exposed in the core of the ridge [*Junger*, 1979; *Vedder et al.*, 1986].

The southwest flank of the northern end of the Santa Cruz-Catalina Ridge is defined by a steep, northwest trending escarpment and a broad uneven terrace that lies about 500–700 m above Santa Cruz Basin (Figure 7). A northwest trending zone of steep faults cuts benches along the escarpment. Numerous slope gullies are evident, and some may be related to slope failures. High-resolution seismic profiles reveal buried, northeast dipping, normal separation faults (Figures 5a and 13 and Figure S3 in the supporting information). Some steep faults show seafloor scarps that represent fault reactivation and basin inversion

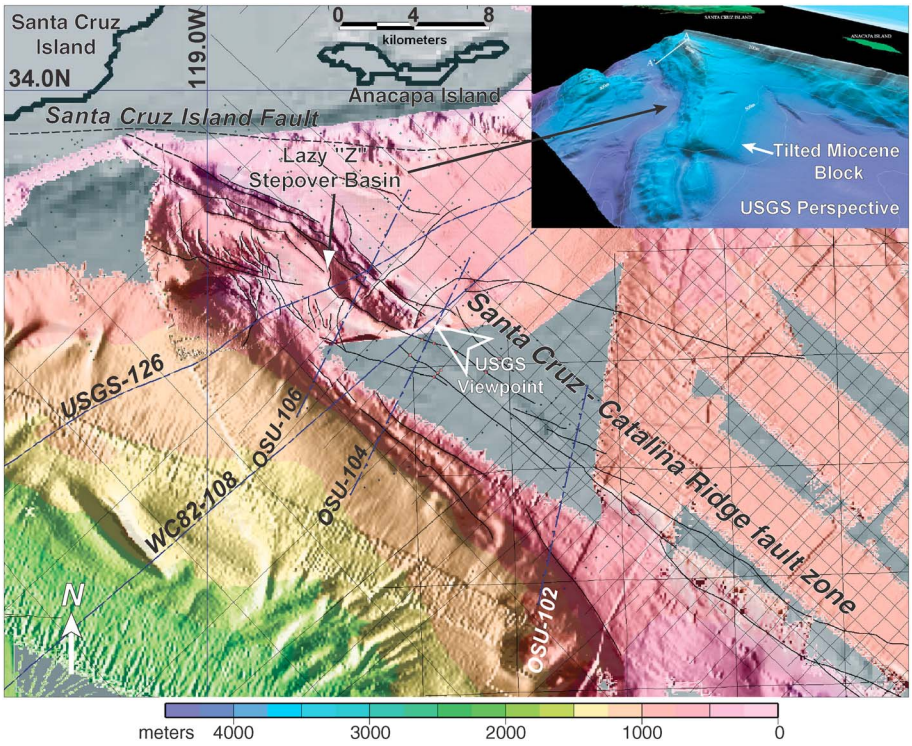

Figure 7. Map showing complex seafloor morphology along the north end of the Santa Cruz-Catalina Ridge where the Borderland meets the western Transverse Ranges. The Santa Cruz-Catalina Ridge fault zone appears to be deflected slightly at the northern end of the ridge but generally maintains its northwest trend all the way to the escarpment south of Anacapa Island (Santa Cruz Island fault after *Chaytor et al.* [2008]). A releasing step over basin (Lazy Z) is located along the principal displacement zone of the Santa Cruz-Catalina Ridge fault zone near the intersection with the west trending escarpment. The dashed blue lines locate MCS profiles shown in Figure S3 in the supporting information (OSU-102, OSU-104, OSU-106, and USGS-126E). Lines USGS-126 and WC82-108 are shown in Figure 13. Inset is perspective view of ridge intersection with Northern Channel Islands platform [*Dartnell et al*., 2005].

with the northeast side uplifted (Figure 5a near SP 410). The complex and irregular East Santa Cruz Basin fault zone lies beneath this terrace [*Bohannon and Geist*, 1998; *Miller*, 2002; *Schindler*, 2010].

4.1.4. Santa Cruz-Catalina Ridge Seismicity

With our more accurate mapping based on the high-resolution bathymetry and seismic reflection profiles presented here, it is possible to evaluate relocations of hypocenters for significant Borderland earthquakes with respect to active faults. Relocated seismicity provides better definition of fault geometry at seismogenic depth and reveals fault connectivity in zones of complex surface deformation [*Graymer et al*., 2007]. Active transpression is expressed in earthquake focal mechanisms that show strain partitioning between right-slip and oblique-reverse movement on subparallel, northwest trending faults (Figure 4). In some cases, the reverse-slip mechanisms involve faults that are oblique to the major strike-slip fault with a west strike subparallel to the Transverse Ranges. For example, the 24 August 2010 (M_L4.0) reverse-slip earthquake struck at depth near Santa Barbara Island while the ALBACORE ocean bottom seismometer array was being deployed. Bathymetry swaths were specifically acquired during that cruise to map the seafloor morphology in the area around Santa Barbara Island.

The 4 September 1981 right-slip Santa Barbara Island earthquake ruptured the Pilgrim Banks segment of the Santa Cruz-Catalina Ridge fault zone with aftershocks that jumped southward to the San Clemente fault [*Corbett*, 1984; *Bent and Helmberger*, 1991] (Figure 6). We plotted the 3-D model-based hypocenter relocations of *Hauksson et al.* [2012] ("HS") in this region for the time period of 1981–2011 to compare with the geological structure and seafloor morphology mapped in this paper. The "preferred" epicenters (Figure 6a) based on the 3-D model and waveform correlations form a tightly clustered lineament (about N53°W) within a broad scatter that plots about 1.5 km to 2.3 km southwest of the mapped principal displacement zone. The 1981 main shock location published by *Corbett* [1984] ("C84") plots along the mapped fault zone near the middle of the aftershock sequence

(Figure 6a). The *Astiz and Shearer* [2000] ("AS") relocated main shock plots about 1 km southwest of the well-defined lineament (Figure 6). The HS main shock is almost 7 km southwest of the mapped fault zone, and there are short, northeast, linear, aftershock trends apparent nearby. One is possibly correlated with a jog in the northwest fault trend near the C84 main shock epicenter (Figure 6a).

The well-defined N53°W trending lineament of aftershocks appears to represent real fault zone geometry mapped in this area including possible segmentation (Figure 6). A southwest trending lineament that ends near the HS main shock may also be real; NE-SW seismicity lineaments are common in Southern California [cf. *Magistrale et al*., 1989; *Magistrale*, 1993] and represent conjugate (or antithetic) faulting as in the Elmore Ranch sequence following the 1987 Superstition Hills, California earthquake [*Magistrale et al*., 1989].

A vertical cross section of the seismicity orthogonal to the fault strike (A-A′ in Figure 6b) reveals a 10 km wide zone with steep-dipping to vertical lineaments, consistent with our fault interpretations based on the high-resolution MCS profiles (Figures 5a and 5b). However, the zone of seismicity is more than twice as broad as the hillside valley. Focal depths are consistent with a seismogenic zone thickness of about 15 km (from 1 to 16 km focal depths) for Southern California strike-slip faults [*Nazareth and Hauksson*, 2004]. The Moho is estimated to be located at 20–22 km depth in this area [*ten Brink et al*., 2000]. The preferred relocations (Figure 6b, black symbols) show a narrow vertical zone (85°SW dip) offset to the west of the mapped principal displacement zone, beneath the escarpment on the southwest flank of the hillside valley located along the projection of the East San Clemente fault. A more diffuse, eastern lineament (80°SW dip) may represent faulting on the other side of this strike-slip basin along the principal displacement zone of the Catalina Ridge fault. Small clusters to the southeast (Figure 6a near profile OSU-128) show interaction or continuity with the East San Clemente fault along the southwest branch at a triple junction. This geometry resembles the San Jacinto fault at Cajon Pass merging with the San Andreas fault (Figure 1). A second cluster farther south is aligned with the northern projection of the San Clemente Island fault southeast of Santa Barbara Island (Figures 4 and 5a). The vertical aftershock zones (Figure 6b) are consistent with the strike-slip focal mechanism of the 1981 earthquake, although seismic reflection profiles show steep-dipping reverse faults in the zone of the step over aftershock cluster (Figure 5c).

Relocated hypocenters of earthquakes associated with the 13 August 1986 offshore Oceanside sequence form a broad elliptical cloud with a northwest trend subparallel to the San Diego Trough fault (Figure 8a). The *Astiz and Shearer*'s [2000] 1-D velocity model waveform-correlated relocations showed a moderate (40°–50°) northeast dip at the base of the seismicity, which *Rivero et al.* [2000] inferred as main shock rupture of the Thirtymile Bank detachment fault, reactivated as a blind thrust. In contrast, the locations using waveform cross correlations and a 3-D velocity model (Figure 8b) [*Hauksson et al*., 2012] show a broad (15–20 km width), vertical zone of activity to depths exceeding 30 km. The various main shock focal depths are shallower than about 10 km (Figure 8b) and near the projected Thirtymile Bank detachment fault.

The 1986 Oceanside main shock and long-lived aftershock sequence have been correlated with a left (restraining) bend in the dextral San Diego Trough fault [*Hauksson and Jones*, 1988; *Ryan et al*., 2012]. The hypocenters from the 3-D model indicate a vertical zone that extends beneath the projected detachment, constrained between the San Diego Trough and Coronado Bank fault zones. Our interpretation of the multichannel seismic profile across the epicenter shows a complex, steep-to-vertical zone of faulting associated with the San Diego Trough fault and steep normal separation faults which offset the Thirtymile Bank detachment fault (Figure 9).

4.2. Ferrelo Fault Zone

The Santa Rosa-Cortes Ridge is one of the largest physiographic features in the California Continental Borderland [*Uchupi*, 1961]. The ridge extends southeast along the axis of the Outer Borderland, from Santa Rosa Island past San Nicolas Island and beyond Cortes Bank for a distance exceeding 220 km (Figures 1 and 10). A well-defined topographic lineament along the west flank of the Santa Rosa-Cortes Ridge (Figures 1, 10, 11, and 12) was identified as a major fault by *Shepard and Emery* [1941]. Renamed the Ferrelo fault [*Junger*, 1979; *Vedder*, 1987], it parallels the structural boundary between the subduction complex rocks of the Patton terrane and the fore-arc basin rocks of the Nicolas terrane [*Howell and Vedder*, 1981]. Our mapping defines the principal displacement zone from Santa Rosa Island to Velero Basin which exceeds 350 km in overall length (Figure 10 and Table 3).

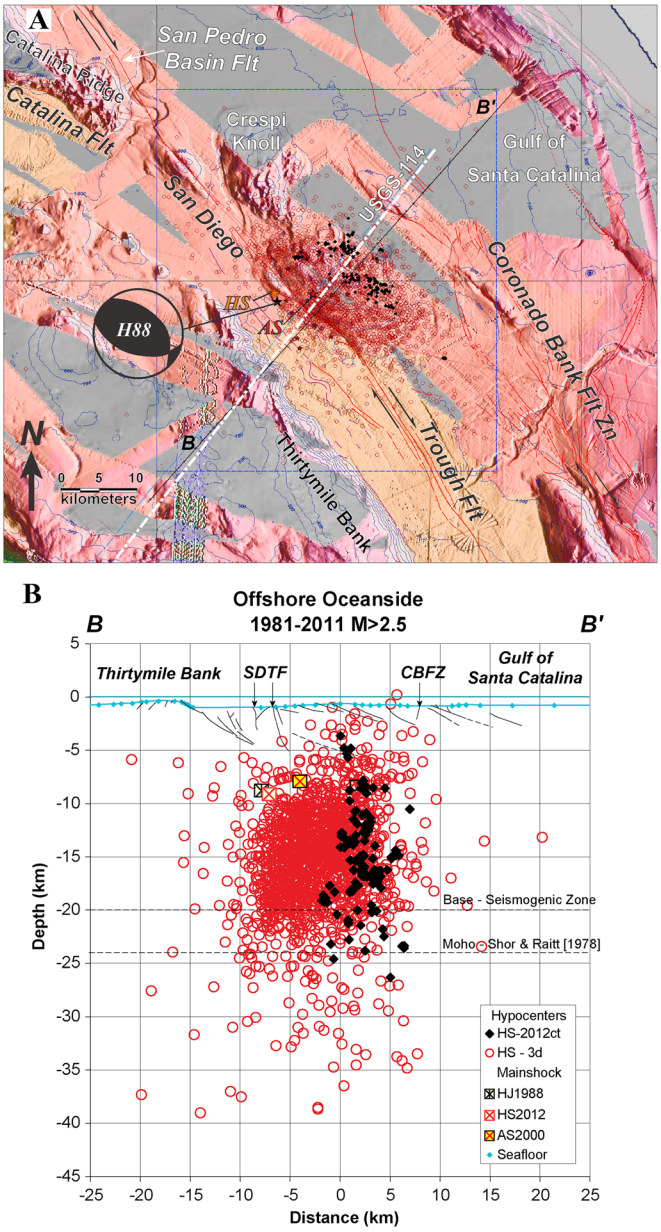

Figure 8. Faulting and seismicity at the southern end of the Santa Cruz-Catalina Ridge where the San Diego Trough fault splits into the Catalina and San Pedro Basin fault zones. The 13 July 1986 $M_s = 5.8$ offshore Oceanside earthquake with sustained aftershock activity displays the complex interaction between high- and low-angle faulting within the Inner Borderland Rift. (a) Map showing relocated seismicity. The brown circles are relocations by *Hauksson et al.* [2012] based on a 3-D model. The black dots are preferred locations using waveform correlations. Main shock locations are shown by boxed stars (HS for *Hauksson et al.* [2012] and AS for *Astiz and Shearer* [2000]). The blue box shows region of seismicity plotted on the map and on cross-section B-B′. Focal mechanism (H88) is from *Hauksson and Jones* [1988]. Faults in the San Diego Trough and Gulf of Santa Catalina are from *Legg* (unpublished mapping and *Nicholson et al.* [1993]). (b) Cross section of seismicity projected onto profile B-B′. The symbols are as described in map above with crosses showing main shock locations from three relocation studies [*Hauksson and Jones*, 1988; *Astiz and Shearer*, 2000; *Hauksson et al.*, 2012]. Background interpreted seismic profile (depth section at no vertical exaggeration) shows low-angle faulting associated with the Thirtymile Bank detachment and middle Miocene rifting of the Inner Borderland and high-angle faulting associated with the San Diego Trough and Coronado Bank fault zone (after *Nicholson et al.* [1993]). Hypocenters relocated by *Astiz and Shearer* [2000] were suggested to delineate the deeper detachment faulting, whereas the 3-D model relocations of *Hauksson et al.* [2012] appear to show a broad zone of seismicity between the subvertical strike-slip San Diego Trough and Coronado Bank fault zones. Earthquakes in California with reverse-fault mechanisms are often associated with broad zones of aftershock seismicity (1987 Whittier-Narrows, 1989 Loma Prieta, and 1994 Northridge). Well-located hypocenters with focal depths deeper than 20 km may be near the Moho.

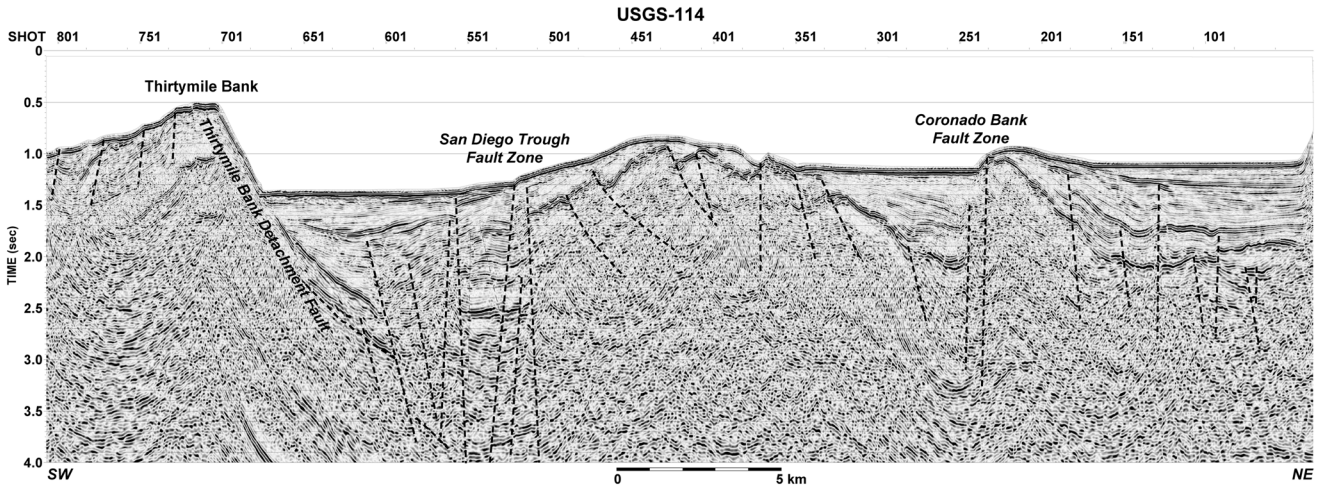

Figure 9. USGS-114 profilen Migrated 44-channel seismic profile across the northern San Diego Trough fault zone (see Figure 8a for profile location). Complex deformation including low-angle detachment (blind thrust?) and high-angle strike-slip (oblique-slip?) faults is evident. The hypocenter of the 1986 main shock is near the intersection of the Thirtymile Bank detachment and San Diego Trough fault zone below the area imaged in the seismic reflection data (seismic processing by *C. Sorlien* [2002]).

4.2.1. Ferrelo Fault Zone Geometry

We covered three major sections of the Ferrelo fault zone with our 2010 ALBACORE multibeam data (Figure 3). High-resolution bathymetry coverage of the Outer Borderland where seismic coverage is less complete than in the Inner Borderland (Figure 11) vastly improved interpretations of active faulting and helped to identify potential sources of seafloor deformation. This analysis better defined the fault pattern as expressed on the seafloor with subsurface confirmation provided by seismic reflection data where available (Figures 12 and 13 and Figure S1 in the supporting information).

The major fault sections recognized along the Ferrelo fault zone are (Figure 10) (i) the north section which extends south ~50 km from the west side of Santa Rosa Island and includes at least two subparallel faults, (ii) the middle section which extends at least 80 km along the western edge of the San Nicolas Island shelf into the Santa Rosa-Cortes Ridge, and (iii) the south section which extends at least 140 km southeast toward Velero Basin and into Mexican waters. A right stepping en echelon pattern appears within some sections with individual fault traces offset by 2–5 km. Also, the overall pattern of the three major sections is right stepping. Based on its straight trend across the area of high topographic relief, like the San Clemente fault to the east, the Ferrelo fault is interpreted as a strike-slip fault [*Shepard and Emery*, 1941]. The Ferrelo fault zone bisects the Outer Borderland and represents one of the largest active fault structures in the region [*Shepard and Emery*, 1941; *Vedder*, 1987].

In the north, the Ferrelo fault zone follows the southwest flank of the Santa Rosa-Cortes Ridge (Figures 3a and 10). The shallow water in the northern section limits the bathymetry swath width so that much of the complex fault pattern mapped is based on the interpretations of seismic profiles [*Junger*, 1979; *Vedder et al.*, 1986; *Schindler*, 2010]. Some well-defined scarps and benches appear in our multibeam data on the steep flank of the broad ridge (Figures 3a and 11). A broad saddle in the crest of the Santa Rosa-Cortes Ridge corresponds to a gentle right bend in the fault zone, but no significant cross-cutting structure has been mapped in this area where dense seismic data are available [*Vedder et al.*, 1986; *Schindler*, 2010]. Northeast trending faults are mapped on the eastern flank of the ridge near the saddle (Figure 10) [*Field and Richmond*, 1980]. The Ferrelo fault zone follows a narrow linear valley across the southwest corner of the San Nicolas Island platform, where Nidever Bank forms a linear ridge on the southwest (Figures 10 and 11). Right (releasing) step overs along the fault zone exist where north to northeast trending escarpments and troughs produce a Lazy Z pull-apart basin east of Nidever Bank.

The prominent west trending San Nicolas Island escarpment and fault zone intersect the Ferrelo fault zone near the middle of the narrow valley (Figure 11). The San Nicolas Island escarpment and fault have a prominent bend near the southeast corner of the island where the western section turns northwest

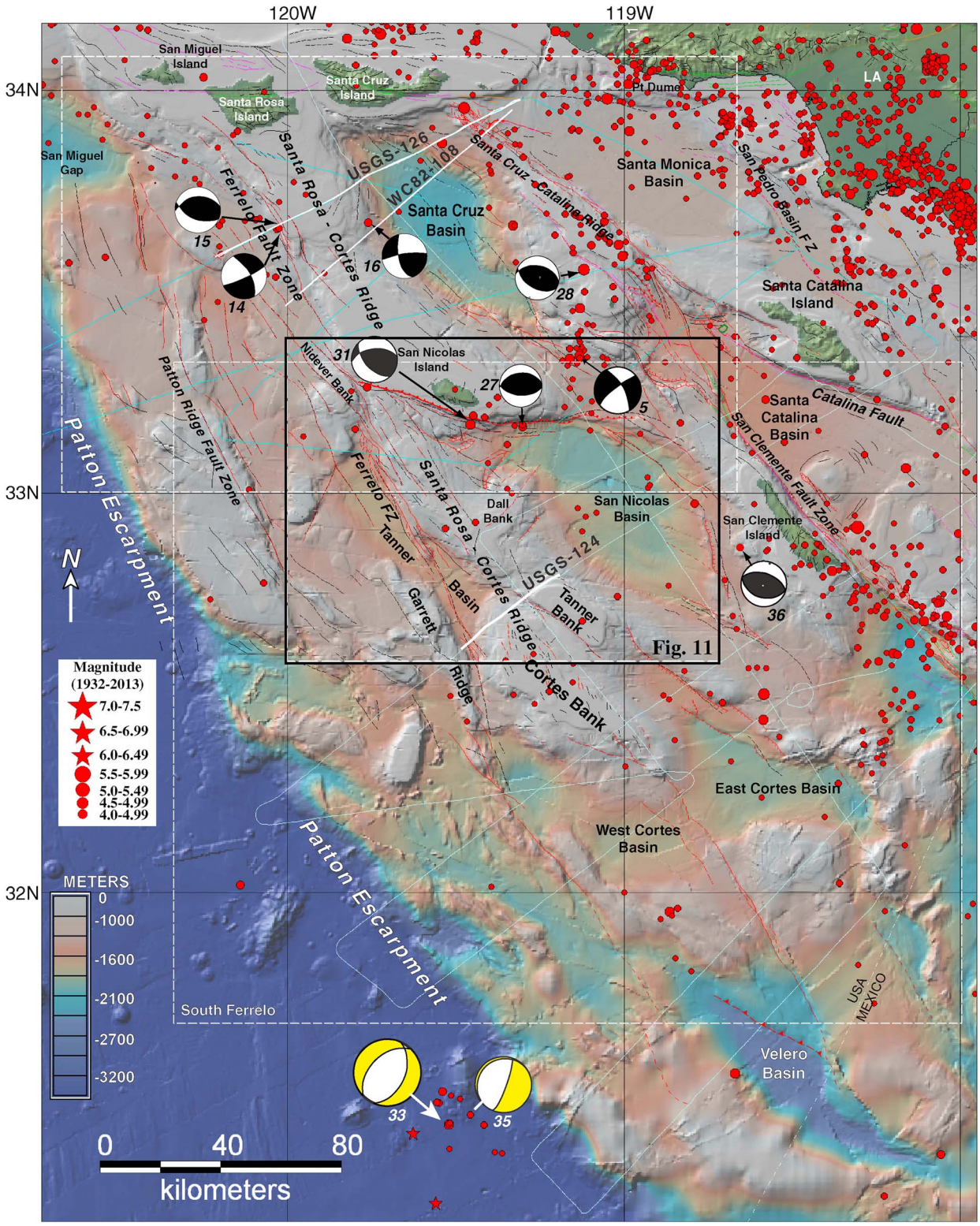

Figure 10. Map showing bathymetry, Quaternary faults, and recent seismicity in the Outer Borderland. Fault locations are based on the high-resolution bathymetry, available high-resolution seismic reflection profiles, and published fault maps [cf. *California Geological Survey* (*CGS*), 2010]. The red symbols show magnitude-scaled ($M > 4$) epicenters for seismicity recorded for the period of 1932 to 2013. Seismicity data and focal mechanisms are derived from the Southern California Seismograph Network catalogs, *National Earthquake Information Center* [2012–2013], and *Legg* [1980]. Focal mechanism event numbers correspond to Table S2 in the supporting information. The black rectangle shows location of Figure 10. The light blue lines show tracklines of multichannel seismic profiles—the labeled white profiles are shown in Figures 12 (124) and 13 (108 and 126). Base map is from GeoMapApp/GMRT [*Ryan et al.*, 2009].

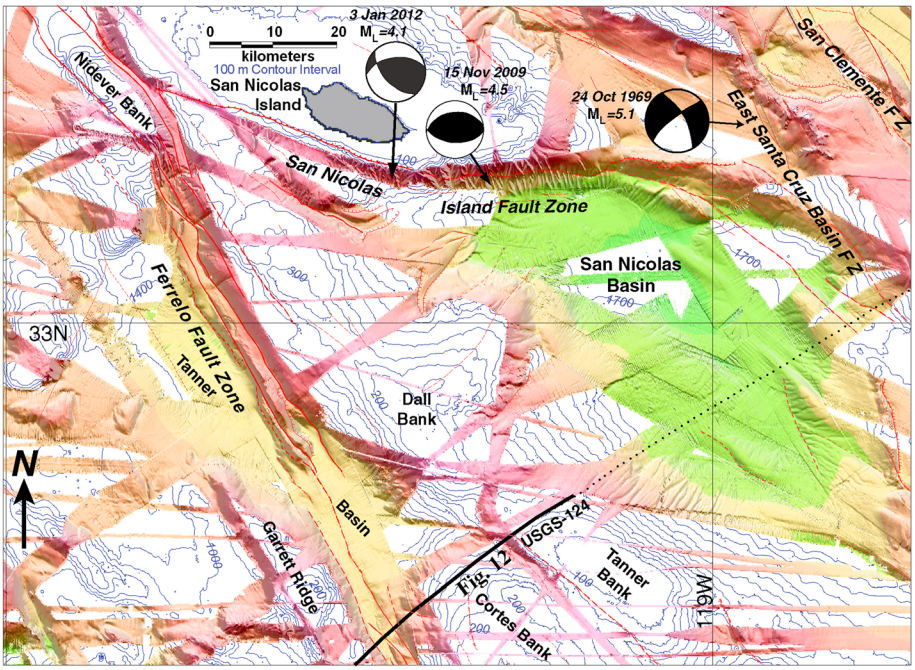

Figure 11. Map showing the seafloor morphology of the Ferrelo fault zone and the intersection with the San Nicolas Island fault zone. The Ferrelo principal displacement zone steps to the right (releasing for right slip) at Tanner Basin and at the San Nicolas Island fault zone, but Nidever Bank appears to represent a local pressure ridge between two more west trending fault traces. The color scale for multibeam bathymetry is same as in Figure 3. See Figure 4 for location of map. The dotted line shows track line of USGS MCS profile 124 (Figure 12).

(N73°W) for a distance of 37 km before intersecting the Ferrelo fault zone. The San Nicolas Island fault zone merges with the East Santa Cruz Basin fault zone to the east [*De Hoogh*, 2012]. The eastern end of the escarpment bends south (S77°E) for about 32 km before intersecting the East Santa Cruz Basin fault zone similar to the west end of the escarpment (Figure 11).

We mapped a major right step over (offset in two 5 km steps) in the Ferrelo fault zone southwest of San Nicolas Island, where the Santa Rosa-Cortes Ridge has another saddle and embayment along its west flank (Figures 10 and 11). Based on the few narrow multibeam swaths available, we imaged several pronounced seafloor lineaments in the area south of Nidever Bank that represent a complex zone of faulting (Figure 11). The coverage improves to the south in Tanner Basin, where multiple scarps and faulted sediments in seismic profiles were identified (Figures 10 and 11) [*Vedder et al.*, 1986].

To the south in the eastern Tanner Basin, the Ferrelo fault system splits into two major zones (Figures 10 and 11). The main zone (Ferrelo) follows the east flank of Garret Ridge on the same trend as the northern section (S70°E), whereas the east branch (Tanner) follows the southwest flank of Tanner Bank on a more easterly trend (S50°E) (Figures 10 and 11). Complex seafloor morphology on the southwest flank of Dall Bank may delineate the east branch that continues southeast through a linear valley between Tanner and Cortes Banks (Figure 11). Tanner Basin is split by the Ferrelo fault zone, and we estimate that about 30 km of right slip would produce the observed offset of the west subbasin relative to the east subbasin (Figures 11 and 14).

The southern section of the Ferrelo fault zone continues to follow the east flank of a broadly sinuous ridge along the west end of West Cortes Basin (Figure 10). This more northerly trend of the ridge and fault in this section, and the basin to the east is consistent with a releasing step over on a right-slip fault zone. Large gaps in the bathymetry data coverage to the south preclude accurate fault mapping, but the fault follows a scarp on the southwest flank of a small linear ridge at the southwest corner of West Cortes Basin (Figure 10). Another fault branches to the southeast along the southern flank of Cortez Bank to link with a northwest trending fault along the west flank of Velero Basin (Figure 10). The escarpment along the northeast flank of Cortes Bank may follow a western branch of the Tanner Bank fault.

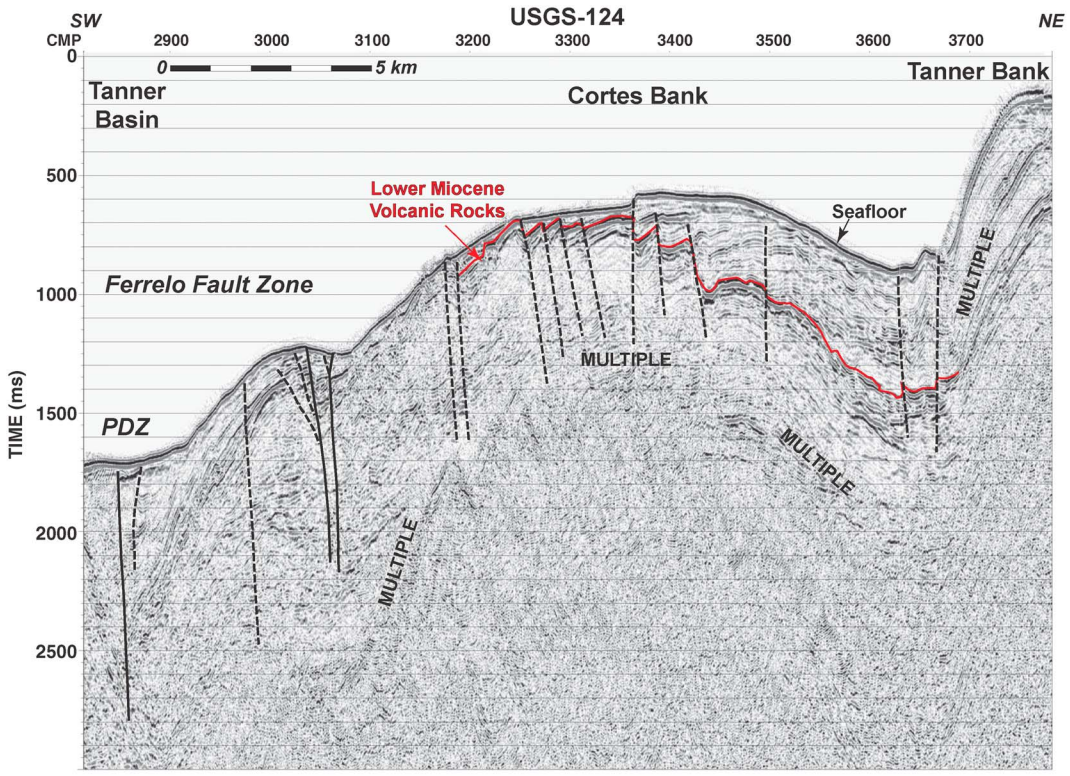

Figure 12. Multichannel seismic reflection profile USGS-124 across the Ferrelo fault zone at the north end of Cortes Bank (see Figure 11 for location). The principal displacement zone for the Ferrelo fault is interpreted to follow the linear valley at the base of the ridge (Tanner Basin). Hillside valleys on the flank of the ridge also follow major fault traces. A set of northeast dipping normal separation faults beneath Cortes Bank demonstrates the inversion of a Miocene basin which appears thickest on the northeast flank of Cortes Bank and continues up the southwest flank of Tanner Bank. Some of these faults are mapped as Quaternary [*Vedder et al.*, 1986; *CGS*, 2010]. (Seismic profile was migrated using a constant velocity of 1460 m/s.)

4.2.2. Ferrelo Fault Zone Seismicity

Fewer epicenters are located along the Ferrelo fault zone in the Outer Borderland than to the east (Figure 10). The lower mapped activity is partly due to the greater distance from the mainland and the seismometers of the Southern California Seismic Network; however, the seismicity catalog is reasonably complete for moderate earthquakes ($M \geq 4$) [*Hutton et al.*, 2010]. Few focal mechanisms are available due to poor azimuthal coverage of seismograph recordings, but as observed along the Santa Cruz-Catalina Ridge, there is a combination of both strike-slip and reverse-slip earthquakes. This is consistent with strain partitioning along transpressional fault zones. Two reverse-slip earthquakes along the San Nicolas Island escarpment (Figure 11) suggest the presence of an active thrust fault along this transverse feature. A north dipping reverse fault is consistent with the uplift of the island and ridge to the north of the escarpment and resembles faulting within the western Transverse Ranges. The event immediately south of the island where the escarpment bends about 10° to the north shows that the bend exists at the earthquake focal depth (Table S2 in the supporting information).

A small cluster of earthquakes in 2005 flanking the northern Santa Rosa-Cortes Ridge (Figure 10) shows the strain partitioning associated with transpression. The event adjacent to Santa Cruz Basin shows right slip on a north-northwest trending focal plane. However, the strike-slip event on the west side of the ridge expresses left slip on the northwest trending focal plane. The reverse-slip focal mechanism is similar to the San Nicolas Island and Santa Barbara Island earthquakes with west trending focal planes.

Seismicity extends south along the Ferrelo fault zone for more than 400 km including activity around Velero Basin (Figure 10). Numerous epicenters are mapped around Cortes and Tanner Banks and farther to the southeast along the faults that branch from the Ferrelo fault zone at Tanner Basin. A roughly linear,

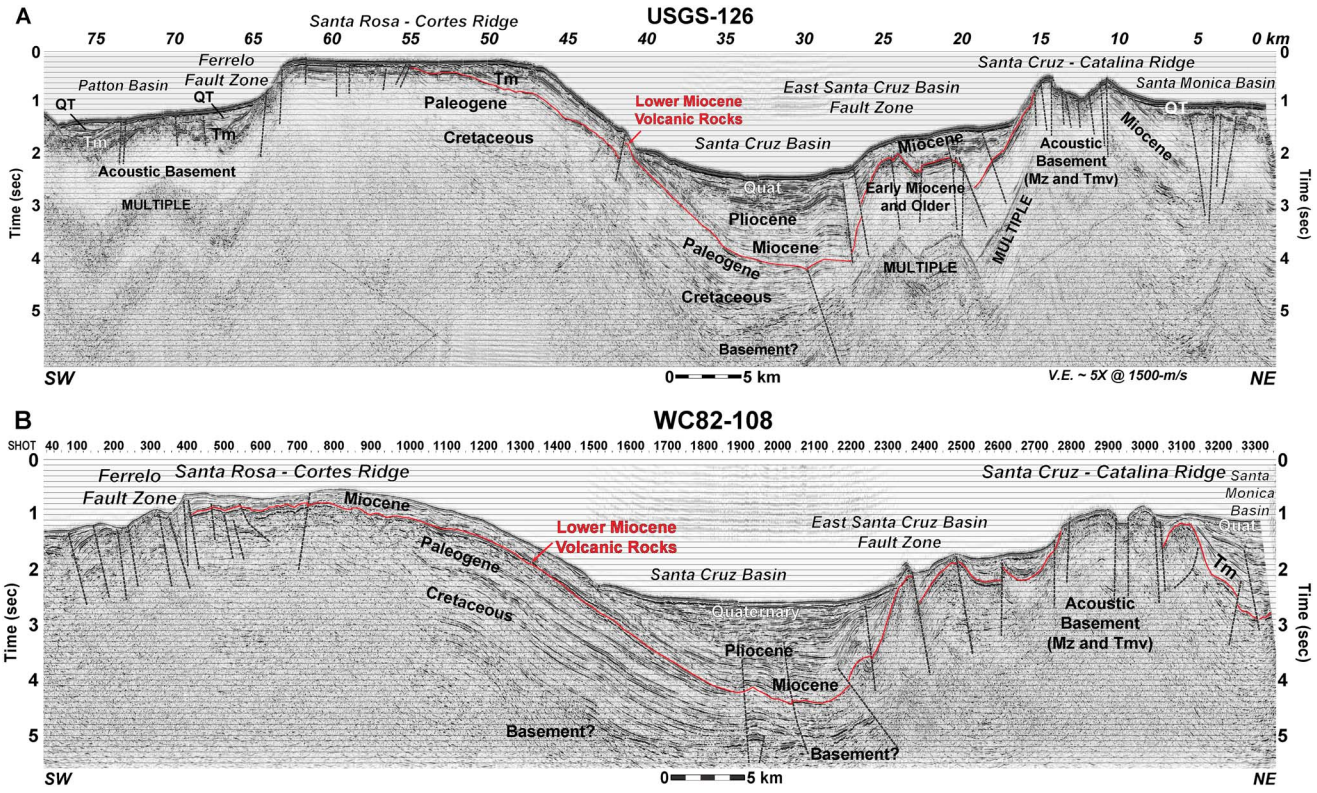

Figure 13. Multichannel seismic reflection profiles across the Northern Borderland show the subsurface geology of the Ferrelo and Santa Cruz-Catalina Ridge fault zones. See Figure 10 for profile locations. The broad, rounded uplift of the Santa Rosa-Cortes Ridge involves Paleogene and Cretaceous sedimentary rocks of the Patton (fore arc) terrane. The complexly faulted, irregular uplift of the Santa Cruz-Catalina Ridge involves Catalina Schist and Miocene volcanic basement rocks with an overburden of Miocene sedimentary rocks. Thin cover of Quaternary sediments exists in small pockets on the ridge crests and along the flanks where the young sediments thicken within the adjacent basins. **QT** = Plio-Pleistocene sediments, **Tm** = Miocene sediments, **Tmv** = Miocene volcanic rocks, and **Mz** = Mesozoic rocks (Catalina Schist).

north-northwest trend to the north of East Cortes Basin includes larger events that represent activity along the East Santa Cruz Basin fault zone which separates the Nicolas fore-arc terrane from the Inner Borderland Rift [*Howell and Vedder*, 1981; *Bohannon and Geist*, 1998; *DeHogh*, 2012]. These events in the southern part of the Outer Borderland are too small and distant for confident determination of their focal mechanisms, so the slip character must be inferred from seafloor morphology (Figure 11), fault trend, and relationship to the regional structure and tectonic framework. Seismic reflection data provide evidence of the vertical component of deformation which appears typical for strike-slip fault zones with both extensional and convergent deformation [*Wilcox et al*., 1973; *Harding*, 1985; *Christie-Blick and Biddle*, 1985; *Sylvester*, 1988; *Legg et al*., 2007] on steep-dipping to vertical faults (Figures 12 and 13).

5. Discussion

5.1. Transpressional Environment

We have described two major transpressional fault zones in the California Continental Borderland—Santa Cruz-Catalina Ridge and Ferrelo. Both are laterally extensive (>100 km), northwest trending zones of convergent right-lateral strike slip (Figure 14). Substantial right slip along northwest trending Borderland fault zones is manifested in dextral offset of large-scale geomorphic features that were created during the middle Miocene and later tectonic evolution of the California Continental Borderland. The rim of the Emery Knoll (EK) crater is offset about 60 km by right slip on the San Clemente fault (Figures 4 and 14) [*Legg et al*., 2004]. Oblique dextral rifting of the San Diego Trough by about 30 km separates Thirtymile Bank from Coronado Bank (Figure 14) [*Legg*, 1991]. A narrow triangular block along the southwest flank of Catalina Ridge (Figure 6) is offset about 20 km from the Farnsworth Bank step over of the Catalina fault, leaving a gap that may represent an elevated pull-apart basin (Figures 4 and 14) [*Legg et al*., 2007]. Tanner

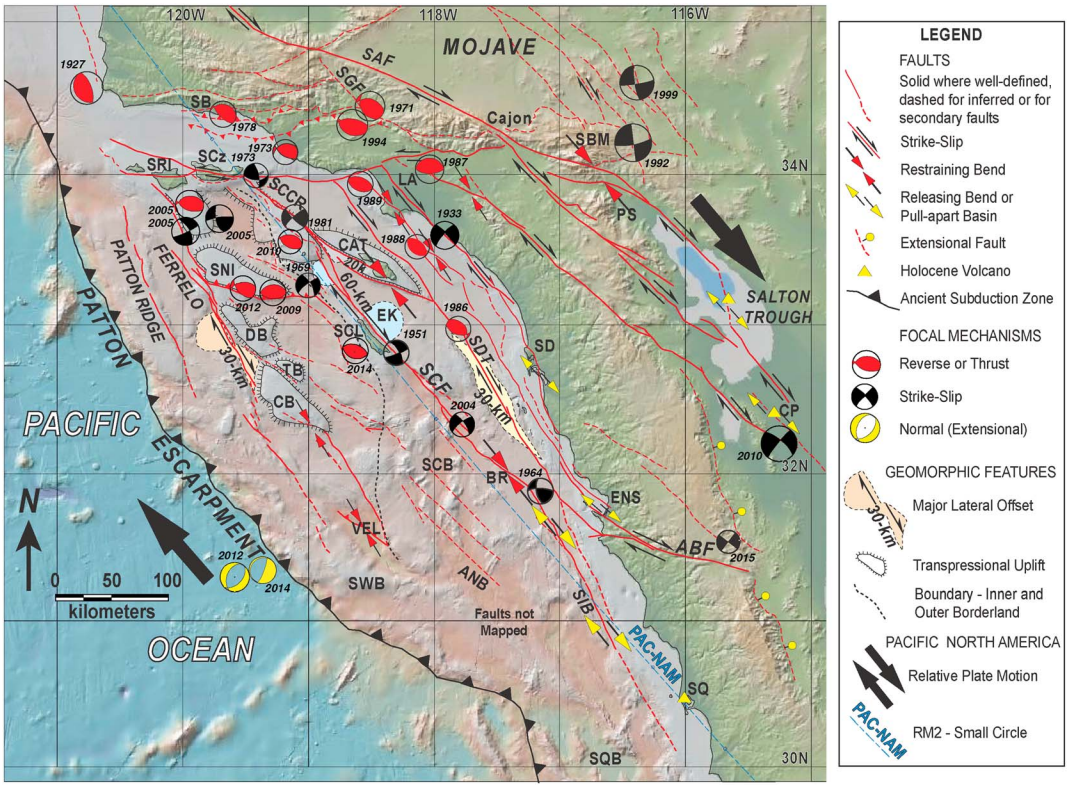

Figure 14. Map showing major active tectonic elements of the northern part of the California Continental Borderland. Major active (Quaternary) faults are shown in red (SAF = San Andreas fault, ABF = Agua Blanca fault, SCF = San Clemente fault, and SCCR = Santa Cruz-Catalina Ridge, Ferrelo). Major strike-slip offsets are shown by shaded areas with estimated displacement (EK = Emery Knoll crater; Tanner Basin near DB = Dall Bank; and SDT = San Diego Trough, small pull-apart near Catalina). Other symbols show oblique fault character including transpressional restraining bends (CAT = Santa Catalina Island, CB = Cortes Bank, and TB = Tanner Bank), uplifts (SRI = Santa Rosa Island, SCz = Santa Cruz Island, SNI = San Nicolas Island, CB = Cortes Bank, TB = Tanner Bank, and SBM = San Bernardino Mountains), and transtensional pull-apart basins (SD = San Diego, ENS = Ensenada, SCB = San Clemente Basin, and SIB = San Isidro Basin). The large arrows show Pacific-North America relative plate motions with the blue dashed line (PAC-NAM) along a small circle for the RM2 [*Minster and Jordan*, 1978] plate motions model through San Clemente Island (SCL). Boundary between the Inner and Outer Borderland follows the East Santa Cruz Basin fault zone (dotted line; modified from *Schindler* [2010] and *De Hoogh* [2012]). Holocene volcanoes exist along the coast (SQ = San Quintín) and within the Gulf of California Rift (CP = Cerro Prieto and Obsidian Buttes, Salton Trough). Dates show year of earthquakes with mapped focal mechanisms (see Table S2 in the supporting information). SB = Santa Barbara, LA = Los Angeles, and PS = Palm Springs.

Basin (Figures 11 and 12) is bisected by the Ferrelo fault and is offset by about 30 km of right slip west of Dall Bank (Figure 14). Streams on the southwest side of Santa Catalina Island are deflected to the northwest consistent with right-lateral shear on the Catalina Ridge fault (Figure 4) [*White et al.*, 2004]. Other geological evidence of right slip includes restraining bend pop-ups along left bends (more west trending than the plate motion vector) and transtensional sag or pull-apart basins at releasing bends and fault step overs (Figure 14) [*Legg*, 1985; *Legg et al.*, 2007]. Focal mechanisms of numerous, small to moderate earthquakes confirm that right slip continues during present time along the major northwest trending fault zones (Figures 4, 5, 10, and 14).

Fault-normal shortening (convergent component of transpression) is manifested in the large-scale morphology of the uplifted ridges—Santa Cruz-Catalina and Santa Rosa-Cortes—that border the major fault zones (hachured areas of Figure 14). Seismic reflection profiles confirm that these ridges are the uplifted flanks of Miocene basins (Figures 5, 12, and 13). The principal displacement zone of each transpressional fault system lies on one side of the elongated basin that was inverted by Pliocene to Recent convergence (Figures 5, 12, 13, and 14). Fault trace irregularities, bends, and step overs along the faults correlate to the transverse boundaries between the major blocks. Branch or secondary faults are part

of this segmentation, particularly in the Outer Borderland along the Santa Rosa-Cortes Ridge. In the Inner Borderland, the Catalina fault branches to the southeast from the longer (>300 km) San Clemente fault zone.

Vertical deformation appears most intense near (<5 km) the principal displacement zone of the Santa Cruz-Catalina Ridge fault system (Figure 14). The broadest area of uplift and highest elevations are associated with the fault segments that are most convergently oblique to the current relative plate motion vector (Pacific-North America (PAC-NAM); Figure 14). The Catalina Escarpment segment is about 33° oblique to the plate motion vector, the Catalina Ridge segment is about 26° oblique, and the northern section including Pilgrim Banks is about 16° oblique (Figure 4). Consistent with variations along the San Andreas fault [*Spotila et al.*, 2007], the uplift pattern represents strain partitioning adjacent to a weak strike-slip fault. Simple shear with right slip on the vertical Santa Cruz-Catalina Ridge and East San Clemente faults is demonstrated by the 1981 Santa Barbara Island earthquake sequence (Figure 6). Pure shear along the flanks of the fault zone produces vertical uplift of the Catalina Schist and igneous basement rocks along the ridge (basement-controlled transpression [*Sylvester and Smith*, 1976]) and forms a large-scale pressure ridge which tilts and folds the adjacent Miocene basin sediments (Figures 5 and 13). The linear hillside valley from Pilgrim Banks to Catalina Ridge (Figures 4 and 5) may represent local extension due to interaction between the East San Clemente and Catalina Ridge faults. The Santa Catalina Island segments (Figure 4) represent a "sharp restraining double bend" [*Crowell*, 1974] linking the Santa Cruz-Catalina Ridge fault zone to the San Diego Trough fault zone [*Legg et al.*, 2004] which resembles the San Bernardino Mountains segment of the San Andreas fault (Figure 14).

Earthquakes with reverse slip along the fault zones and adjacent ridges indicate active regional strain partitioning with strike-slip earthquakes occurring on the steep to vertical faults which flank the uplifted crustal blocks (Figures 4, 5, 10, and 14). Southern California strain partitioning was proposed [*Nicholson and Crouch*, 1989] based on clustering of strike-slip earthquake focal mechanisms along the major active vertical faults which separated zones of reverse or thrust earthquakes on low-angle fault planes subparallel to the strike-slip faults. Conceptual models suggested that the strike-slip faults terminate or are offset by the low-angle fault planes [*Rivero et al.*, 2000]. However, along the Santa Cruz-Catalina Ridge fault zone, the vertical fault zone active during moderate earthquakes extends through the entire seismogenic zone (Figure 6b). The Santa Cruz-Catalina Ridge may be a transform fault exhibiting simple shear parallel to the current relative plate motion (Figure 14) as recognized for the San Clemente-San Isidro fault zone [*Legg*, 1985; *Legg et al.*, 1989; *Legg*, 1991].

Vertical deformation along the Santa Rosa-Cortes Ridge is manifested in a 215 km long × 30 km wide anticlinorium consisting of several large uplifted anticlinal blocks (Figures 10 and 14) [*Vedder*, 1987]. The west-northwest fold trends are convergently oblique to the Ferrelo fault zone and were considered to form in simple shear across the broad Pacific and North American transform plate boundary [*Vedder*, 1987]. Broadest uplift and highest elevations correspond to the blocks with the most convergent trend, such as San Nicolas Island and Cortes Bank (Figures 10, 11, and 14). The uplift and convergent deformation appears to decrease to the east (farther from the Ferrelo fault zone), where the major basins exist (Santa Cruz, San Nicolas, and East Cortes; Figure 10) [*Vedder*, 1987]. This pattern may represent strain partitioning as described above on the Santa Cruz-Catalina Ridge and San Andreas fault zones; however, the Ferrelo fault zone trend is N25°W—about 15° divergently oblique to the PAC-NAM relative motion (Figure 14). A clockwise rotation of the regional (plate boundary) maximum principal stress orientation may be required to produce northeast directed shortening on the Santa Rosa-Cortes Ridge [e.g., *Nur and Ron*, 2003]. This stress rotation may correspond to the observed late Miocene clockwise rotation of the displacement vector for the Pacific plate [*Atwater and Stock*, 1988].

Alternatively, north directed shortening evident in the western Transverse Ranges (Figure 14; e.g., 1973 Point Mugu and 1987 Whittier-Narrows (Los Angeles (LA)) earthquakes) may be propagating southward by telescoping of the Santa Rosa-Cortes Ridge. Transverse faults along the San Nicolas Island platform (Figures 10, 11, and 14) exhibit north directed convergence and thrust faulting. Reverse slip on west trending fault planes is evident in earthquake focal mechanisms between the Ferrelo fault zone and the Santa Cruz-Catalina Ridge–San Clemente fault zones (Figures 10 and 14). In contrast, the 1986 Oceanside earthquake at the north end of the San Diego Trough shows reverse slip on northwest trending focal planes (Figures 4, 8, and 14). We infer that this represents northeast directed shortening similar to that of the 1927 Lompoc earthquake (Figure 14) and other earthquakes in the Coast Ranges surrounding the San Andreas fault in central California (e.g., 1983 Coalinga earthquake [*Helmberger et al.*, 1992]).

Timing of significant tectonic deformation is loosely constrained by available data, but we infer that the larger offset features formed during the middle Miocene oblique rifting of the Inner Borderland [*Legg*, 1991]. Holocene volcanoes along the Baja California coast at San Quintín and within the Gulf of California extensional province (Figure 14) demonstrate that active extension persists on both sides of the Peninsular Ranges. Transtension associated with large pull-apart basins at San Diego Bay and Todos Santos Bay (Ensenada) and structural sags along N30°W fault trends (San Isidro Basin; Figure 14) involves offset of late Quaternary sediments imaged in high-resolution seismic profiles [*Kennedy and Welday*, 1980; *Legg*, 1985; *Legg et al*., 1991]. Basin inversion along the major transpressional fault zones (Ferrelo and Santa Cruz-Catalina Ridge) appears to be post-Miocene as middle to late Miocene basin sediments are uplifted along the flanks and within the pop-up structure itself (Figures 5, 12, and 13) [*Uchupi*, 1961; *Vedder et al*., 1974; *Junger*, 1979; *Crouch*, 1981; *Howell and Vedder*, 1981; *Miller*, 2002; *Schindler*, 2010]. Pliocene strata with divergent dips are elevated along the ridge flanks and record ridge growth [*Junger*, 1979]. Uplift diminished as late Quaternary sediments are draped on the slope above the tilted sequences of Pliocene deposits. At the northwest corner of Santa Monica Basin, folded and faulted late Quaternary sediments [*Normark et al*., 2004] lap onto tilted late Miocene basin fill and are tilted up on the Santa Cruz-Catalina Ridge flank south of Anacapa Island (Figure S3 in the supporting information).

Convergent right-lateral slip (transpression) along faults of the Santa Cruz-Catalina Ridge and Santa Catalina Island zones uplifted the ridge and island following the clockwise rotation of the PAC-NAM relative motion vector [*Atwater and Stock*, 1988]. We estimate that about 1 km of structural relief on the late Miocene horizon, from the wave-cut surface near Pilgrim Banks to the buried horizon in Santa Monica Basin (Figure 5), represents a post-Miocene uplift rate of about 0.1–0.2 m/kyr. This rate is comparable to uplift rates of coastal terraces in Southern California south of the Transverse Ranges [*Lajoie et al*., 1992]. For Santa Catalina Island, the post-Miocene uplift rate was at least double that amount [*Legg et al*., 2004].

Submerged marine terraces around Santa Catalina Island are inferred to demonstrate late Quaternary subsidence [*Castillo et al*., 2012] which is consistent with uplift cessation shown by onlap at the base of flat-lying late Quaternary sedimentary sequences in San Pedro Basin [*Francis et al*., 2013]. Late Quaternary bypass of the Catalina fault restraining bend by linkage between the San Pedro Basin and San Diego Trough faults (Figure 8a) removed a significant component of fault-normal shortening allowing the island and ridge to subside. A similar linkage between the major dextral San Clemente Island fault and Santa Cruz-Catalina Ridge fault zone via a releasing fault bend (Figure 6a) may be responsible for subsidence of the Santa Cruz-Catalina Ridge to the north of this extensional step over. At the northern end of the Santa Cruz-Catalina Ridge where the Inner Borderland collides with the western Transverse Ranges, underthrusting depresses the Santa Cruz-Catalina Ridge producing additional subsidence. Meanwhile, the Northern Channel Islands platform is uplifted as shown by the relative elevation increase of the Last Glacial Maximum terraces on the west trending southern flank of Santa Cruz and Anacapa Island platforms [*Chaytor et al*., 2008].

5.2. Borderland-Baja California Microplate Tectonics

Currently, the Borderland accommodates a significant component (10–25%) of relative plate motion [*Plattner et al*., 2007] on offshore faults. Recent seismicity, including the 14 December 2012 (M_w6.3) earthquake in the Pacific oceanic lithosphere west of the Patton Escarpment, demonstrates that the plate boundary forces may extend across the full 500 km width to this earthquake [*Hauksson et al*., 2013]. A systematic pattern of transpression, north directed at the northern end of the Borderland and northeast directed in the Inner Borderland offshore San Diego, and transtension (oblique extension) in the southern region offshore Baja California (Figure 14), is evidence confirming a model of splintering at the northern end of a long semirigid Baja California microplate [*Legg*, 1985, 1991; *Dixon et al*., 2000; *Plattner et al*., 2007]. The San Clemente fault zone separates two large-scale domains of transpression in the Northern Borderland, acting as a transform fault accommodating most of the right slip between the Baja California microplate and the oceanic Pacific plate to the west. The transpression is limited to the south at the latitude of the trans-Peninsular Ranges Agua Blanca fault, which also exhibits pure right slip [*Allen et al*., 1960] analogous to an intracontinental transform fault.

The Ferrelo fault zone and Santa Rosa-Cortes Ridge have a N25°W–35°W trend, which is 5–15° divergent from the relative plate motion vector (Figure 14). One would expect transtension along the Ferrelo fault zone, and

the right stepping en echelon fault character is consistent with oblique rifting, as in the Gulf of California and Inner Borderland. The distinct uplifted blocks that appear to have restraining fault geometry on their southern edges may represent local restraining bend uplift that combines along the trend of the Ferrelo fault zone to produce the larger Santa Rosa-Cortes Ridge. Nevertheless, the observed transpression manifest as the broad anticlinorium and large-scale basin inversion along the Santa Rosa-Cortes Ridge may involve a clockwise rotation of the regional (Outer Borderland) strain tensor to induce northeast directed convergence along the Ferrelo fault zone.

5.3. Tectonic Logjam

Reverse-slip focal mechanisms on northwest trending "blind" thrust faults and Miocene basin inversion along the Newport-Inglewood and Palos Verdes fault zones in coastal Southern California [*Nicholson and Crouch*, 1989; *Legg*, 1991; *Wright*, 1991; *Crouch and Suppe*, 1993; *Rivero et al*., 2000; *Sorlien et al*., 2013] comprise evidence for regional northeast directed shortening due to the restraining bend in the southern San Andreas fault (Figure 14). Late Miocene clockwise rotation of the PAC-NAM relative motion followed by the jump of the plate boundary to the Gulf of California initiated the Borderland transpression and inverted transtensional basins in the Inner Borderland Rift [*Legg et al*., 2007]. Crustal thickening by uplift of the Transverse Ranges during the Pasadenan orogeny (Figure 2) [*Wright*, 1991] likely involved deepening of the cold subcrustal lithospheric seismic anomaly [*Humphreys and Hager*, 1990; *Kohler*, 1999; *Houseman et al*., 2000] and marked the severity of the collision between the Baja California microplate and the Transverse Ranges. We suggest that this collision decouples the Baja California microplate from the oceanic Pacific plate and produces the varying Borderland transpressional character described above. Historic earthquakes with reverse-slip or thrust focal mechanisms confirm that regional transpression remains active across the Northern Borderland (Figures 4, 10, and 24).

Our observations suggest that offshore deformation can be compared kinematically to a logjam effect. Obstruction to right-lateral slip is imposed by the western Transverse Ranges which appear to shift north directed shortening southward as far as San Nicolas Island which is stuck like a log upstream from a dam. Transpression associated with the logjam kinematics involves uplift of tectonic (crustal) blocks by vertical displacement between and within high-angle faults. Fault triple junctions (see supporting information for more detail) created during the plate boundary evolution create areas of more intense vertical deformation at the ends of elongate fault-bounded crustal blocks (logs in the logjam). The collision of the Borderland and coastal Southern California end of a Baja California microplate against a thickened Transverse Ranges crust and lithosphere is splintering the Borderland into a number of crustal blocks. The block boundaries follow ancient structural discontinuities created by oblique rifting of the margin during the Miocene plate boundary reorganization and are possibly remnant from early Tertiary subduction. Convergence induced by the collision is oblique (transpressional) along northwest trending former transform faults where strain is partitioned into right slip on weak vertical fault zones (simple shear) and fault-normal convergence (pure shear) in adjacent areas of uplift. In addition, convergence may be nearly orthogonal on local west trending structures like the San Nicolas Island escarpment (Figures 10 and 11) consistent with wrench faulting (simple shear [*Wilcox et al*., 1973].

At the Transverse Ranges intersection, right slip must be absorbed on the west side of the northwest trending faults. Folding and thrust faulting exist over a broader area west of the Santa Cruz-Catalina Ridge fault zone than to the east. By contrast, north directed shortening to the east implies that clockwise vertical-axis rotation of the western Transverse Ranges block is insufficient to accommodate northwest translation of the Inner Borderland (Figures 7, 10, and 13). At the north end of the Santa Cruz-Catalina Ridge, the shape of uplift on the northeast flank resembles a ramp or elevated trapdoor bounded by a northeast trending conjugate fault midway along the pop-up (Figure 7). The Miocene sequence on USGS-126 shows subparallel bedding and uniform tilt, whereas on WC82-108, this sequence pinches out on the flank of uplifted acoustic basement (Figure 13 and Figure S3 in the supporting information; OSU-106). The southwest flank of the tilted block is a steep escarpment (up to 450 m high on A-A′ Figure 7 inset) that bounds the step over basin which resembles a "keystone" graben at the crest of an anticline (Figures 7 and 13).

This complex zone of uplift exists where the Inner Borderland intersects the western Transverse Ranges. Northeast directed convergence along the Santa Cruz-Catalina Ridge changes to north directed convergence in the Transverse Ranges. Adjacent zones of folds and reverse faults [*Chaytor*, 2006; *Chaytor*

et al., 2008] accommodate the shortening of the sedimentary deposits and underlying bedrock of the shallow crust. These zones can be compared to complex structure in the Chino Hills, 30–50 km east of Los Angeles, where the Whittier-Elsinore fault zone intersects the western Transverse Ranges.

5.4. Earthquake Potential

Our analysis indicates that the major transpressional fault systems of the Borderland may produce large earthquakes ($M > 7$) that include strike-slip or reverse-slip deformation. The largest recorded earthquake in the California Continental Borderland region was the 4 November 1927 Lompoc earthquake ($M_s = 7.0$; Figure 14) which had a reverse focal mechanism [*Helmberger et al*., 1992] and generated a small tsunami (~2 m) [*Satake and Sommerville*, 1992]. Both transpressional fault systems investigated here are long (>300 km) and complex. In general, the principal displacement zones are narrow (<5 km), consistent with vertical strike-slip fault zones (Figures 5 and 6). The zone of faulting is broad (>10 km), where oblique slip is evident (Figures 7, 11, and 13). Nevertheless, relocated hypocenters along the Santa Cruz-Catalina Ridge (Figure 6) show a vertical shear zone to depths exceeding 16 km. The seismogenic zone as defined by *Nazareth and Hauksson* [2004] extends from 1.8 km to 16 km depth beneath the ridge (Figure 6b), similar to the 14 km elastic fault width estimated beneath Santa Catalina Island [*Legg et al*., 2004]. A moderate fault dip is interpreted from seismic profiles (Figure 13) [*Schindler*, 2010] for the Ferrelo fault zone where earthquake focal depths are poorly constrained. Based on geophysical models of the Outer Borderland [*Miller*, 2002], we assume an average fault width of 10 km for estimation of earthquake potential on the Ferrelo fault zone. We estimated magnitudes for potential large earthquakes along the transpressional fault zones (Table S3 in the supporting information) based on correlations of maximum magnitude versus fault length and area [*Hanks and Bakun*, 2002; *Working Group on California Earthquake Probabilities*, 2003]. Slip rates for the Santa Cruz-Catalina Ridge and Ferrelo fault zones are poorly constrained, but GPS strain measurements are consistent with northwest directed dextral shear of 6–12 km/Ma west of the southern San Andreas-Gulf of California fault zone in northern Baja California [*Plattner et al*., 2007]. During the past 150 years, several large earthquakes have ruptured low-slip-rate faults in areas of extended California crust including the central California Borderland ($M_s = 7.0$, 1927), Owens Valley ($M_w = 7.8$–7.9, 1872), Mojave ($M_w = 7.4$, 1992 and $M_w = 7.1$, 1999), and Laguna Salada ($M_w = 6.8$, 1892 and $M_w = 7.2$, 2010). The major transpressional fault systems of this study may produce events of similar magnitude and fault complexity.

6. Conclusions

Over 4500 line-km of new multibeam bathymetry data combined with existing bathymetry, seismic profile, and seismicity data are used to characterize the geometries of two active transpressional fault zones in the California Continental Borderland, the Santa Cruz-Catalina Ridge fault and the Ferrelo fault. The data show that fault-normal convergence is expressed as large crustal blocks uplifted along these major Borderland transpressional fault systems. The principal displacement zones of these faults flank the uplifts on one side and accommodate mostly strike slip. The scale and character of the uplifts vary and appear to correspond to the degree of convergent obliquity to the principal displacement zone and the tectonic displacement vector. In the Inner Borderland, the Santa Cruz-Catalina Ridge fault zone represents the northern sections of the San Clemente fault system and has convergent obliquity of 17° to 33° relative to the plate motion vector. The largest uplift, the Santa Catalina Island block, has the greatest obliquity. It includes an uplifted pull-apart basin at a releasing step over and represents a rhomboidal pop-up structure on a restraining double bend. The other uplifts along the Santa Cruz-Catalina Ridge exhibit restraining orientations but are considered pressure ridges with metamorphic and igneous basement rocks squeezed upward along the vertical fault zone representative of basement-controlled transpression.

In the Outer Borderland by contrast, the Santa Rosa-Cortes Ridge is a 215 km long, 30 km wide anticlinorium cored by upper Cretaceous to Oligocene fore-arc rocks above an ophiolite basement of the Nicolas fore-arc terrane. The Ferrelo fault zone trend is divergently oblique to the Pacific-North America relative plate motion vector; yet Miocene and older basins have been structurally inverted along the northeast side of the principal displacement zone. Transverse faults along the San Nicolas Island platform exhibit north directed convergence and thrust faulting consistent with simple shear along a dextral northwest trending

transform fault zone. Smaller blocks such as Tanner Bank and Cortes Bank may correspond to local restraining faults along their southwest flanks. However, the axis of the broad anticlinorium is parallel to the Ferrelo fault zone and divergent to the relative plate motion vector.

The San Clemente fault zone separates two large-scale domains of transpression in the Northern Borderland, acting as a transform fault accommodating most of the right slip between the Baja California microplate and the oceanic Pacific plate to the west. The transpression is limited to the south at the latitude of the trans-Peninsular Ranges Agua Blanca fault, which also exhibits pure right slip analogous to an intracontinental transform fault. The northern domain of dextral shear and transpression located east of the San Clemente fault is the Southern California shear zone at the northern end of a possibly splintered Baja California microplate. The Ferrelo fault zone and Outer Borderland domain of dextral shear and transpression continue to the south, as does the San Clemente-San Isidro fault zone where dextral shear and extension persist in the southern Borderland in Baja California.

Reorientation of the maximum principal stress axis from north-south at the Transverse Ranges to northeast-southwest within the Northern Borderland creates pure shear in these large crustal blocks of the Outer Borderland. During late Quaternary to present day, collision of the Borderland crust with the Transverse Ranges has intensified the transpression so that north directed convergence is manifested in west trending reverse/thrust earthquakes along the Santa Rosa-Cortes Ridge and the San Nicolas Island escarpment. Shortening is also manifested on Inner Borderland earthquakes including the 1986 Oceanside earthquake with reverse/thrust faulting on northwest trending focal planes and within a $>$15 km deep zone of vertical deformation. The observations fit a logjam model for offshore deformation; obstruction to northwest directed right-lateral strike slip imposed by the western Transverse Ranges shifts north directed shortening southward as far as San Nicolas Island, through a crustal block consisting of the northern Santa Rosa-Cortes Ridge, which is stuck like a log at a dam in a river. The long ($>$200 km), oblique-motion Santa Cruz-Catalina Ridge and Ferrelo fault zones remain active today and may be capable of large Borderland earthquakes ($M > 7$) with complex fault rupture patterns and tsunamigenic potential.

Acknowledgments

Exploration industry deep penetration seismic profiles released by WesternGeco for research purposes are available in the USGS *NAMSS* [2006] database. U.S. Geological Survey multibeam surveys are available in the *NAMSS* [2006] database and *Infobank* [2013]. The USGS and WesternGeco do not warrant the use of these data nor make any claims or guarantees as to the accuracy of the data identification, acquisition parameters, processing methods, navigation, or database entries. The 2010 ALBACORE R/V *Melville* cruise multibeam bathymetry data will be made available from the NOAA National Geophysical Data Center archive. The raster images of multibeam bathymetry used for this study will be available from the Southern California Earthquake Data Center with file descriptions provided in Table S1 in the supporting information. Chris Goldfinger provided important high-resolution seismic reflection data and several important multibeam bathymetry swaths from prior surveys. Joann Stock provided important multibeam swaths along the southern Ferrelo fault zone that filled important data gaps. Earthquake location parameters for events with focal mechanisms shown in this paper are presented in Table S2 in the supporting information. Seismicity data are available

References

Allen, C. R., L. T. Silver, and F. G. Stehli (1960), The Agua Blanca fault—A major transverse structure of northern Baja California, Mexico, *Geol. Soc. Am. Bull.*, *71*, 457–482.

Astiz, L., and P. M. Shearer (2000), Earthquake locations in the inner Continental Borderland offshore Southern California, *Seismol. Soc. Am. Bull.*, *90*, 425–449.

Atwater, T. (1970), Implications of plate tectonics for the Cenozoic tectonic evolution of western North America, *Geol. Soc. Am. Bull.*, *81*, 3513–3536.

Atwater, T., and J. Stock (1988), Pacific-North American plate tectonics of the Neogene southwestern United States: An update, *Int. Geol. Rev.*, *40*, 375–402.

Bent, A. L., and D. V. Helmberger (1991), Seismic characteristics of earthquakes along the offshore extension of the western Transverse Ranges, California, *Seismol. Soc. Am. Bull.*, *81*, 399–422.

Biddle, K. T., and N. Christie-Blick (Eds.) (1985), *Strike-Slip Deformation, Basin Formation, and Sedimentation*, *Spec. Publ.*, vol. 37, 386 pp., Soc. Econ. Paleontol. Mineral., Tulsa, Okla.

Bohannon, R. G., and E. Geist (1998), Upper crustal structure and Neogene tectonic development of the California Continental Borderland, *Geol. Soc. Am. Bull.*, *110*, 779–800.

Bohoyo, F., J. Galindo-Zaldivar, A. Jabaloy, A. Maldonado, J. Rodriguez-Fernandez, A. Schreider, and E. Surinach (2007), Extensional deformation and development of deep basins associated with the sinistral transcurrent fault zone of the Scotia-Antarctic plate boundary, in *Tectonics of Strike-Slip Restraining and Releasing Bends in Continental and Oceanic Settings*, edited by W. D. Cunningham and P. Mann, *Geol. Soc. London Spec. Publ.*, *290*, 203–217.

Buchanan, J. G., and P. B. Buchanan (1995), *Basin Inversion*, *Geol. Soc. London Spec. Publ.*, *88*, 596.

California Geological Survey (CGS) (2010), *Fault Activity Map of California*, Calif. Geol. Surv., Sacramento, Scale 1:750,000.

Castillo, C. M., R. D. Francis, and M. R. Legg (2012), Constraints on late Quaternary subsidence of Santa Catalina Island from submerged paleoshorelines, AGU, Annual Meeting, San Francisco, Calif.

Chaytor, J. D. (2006), Diffuse deformation patterns along the North American plate boundary zone, offshore western United States, PhD thesis, Oregon State Univ., Corvallis, OR, p. 299.

Chaytor, J. D., C. Goldfinger, M. A. Meiner, G. J. Huftile, C. G. Romsos, and M. R. Legg (2008), Measuring vertical tectonic motion at the intersection of the Santa Cruz-Catalina Ridge and Northern Channel Islands platform, California Continental Borderland, using submerged paleoshorelines, *Geol. Soc. Am. Bull.*, *120*, 1053–1071.

Christie-Blick, N., and K. T. Biddle (1985), Deformation and basin formation along strike-slip faults, in *Strike-Slip Deformation, Basin Formation, and Sedimentation*, *Spec. Publ.*, vol. 37, edited by K. T. Biddle and N. Christie-Blick, pp. 1–34, Soc. Econ. Paleontol. Mineral., Tulsa, Okla.

Corbett, E. J. (1984), Seismicity and crustal structure studies of Southern California: Tectonic implications from improved earthquake locations, PhD thesis, Pasadena, California Institute of Technology, 231 pp.

Crouch, J. K. (1981), Northwest margin of California Continental Borderland: Marine geology and tectonic evolution, *Am. Assoc. Pet. Geol.*, *65*, 191–218.

from the Southern California Earthquake Data Center (www.scedc.caltech.edu/eq-catalogs/) and from *Astiz and Shearer* [2000]. This work was supported by the National Science Foundation grants OCE-0825254 (MDK) and OCE-0824982 (DSW) and the Southern California Earthquake Center (grants 09094, 11100 and 13091, MRL). SCEC is funded by NSF Cooperative Agreement EAR-1033462 and USGS Cooperative Agreement G12AC20038. The SCEC contribution number for this paper is 1742. We are especially grateful to Alexander Densmore, Paul Umhoefer, Luciana Astiz, Kristin Rohr, and an anonymous reviewer for their thoughtful reviews of the manuscript that helped us to describe more coherently this complex area of active deformation. We thank Chris Sorlien for comments on early drafts of the manuscript and for numerous discussions of Borderland tectonics. Marc Kamerling shared many ideas regarding the Borderland tectonic evolution that helped provide the background for this research. Mike Barth insured that the high-resolution multichannel seismic data were of the highest quality during acquisition. Jason Chaytor's dissertation mapping was an important basis for understanding the subbottom geological structure and its correlation to seafloor morphology. The assistance of the Scripps Geological Data Center in coordinating outbound/inbound cruises to cover new Borderland territory with multibeam swaths during the past three decades is greatly appreciated. Kohler and Weeraratne are grateful to Captain Christopher Curl and the entire crew of R/V *Melville* for their assistance and flexibility in accommodating the additional multibeam bathymetry data gathering routes during the 2010 ALBACORE cruise.

Crouch, J. K., and J. Suppe (1993), Late Cenozoic tectonic evolution of the Los Angeles Basin and Inner California Borderland: A model for core complex-like crustal extension, *Geol. Soc. Am. Bull.*, *105*, 1415–1434.

Crowell, J. C. (1974), Origin of late Cenozoic basins in Southern California, in *Society of Economic Paleontologists and Mineralogists (Society for Sedimentary Geology)*, *Spec. Publ.*, vol. 22, pp. 190–204, Tectonics and Sedimentation, Tulsa, Okla.

Dartnell, P., G. R. Cochrane, and M. E. Dunaway (2005), Multibeam bathymetry and backscatter data: Northeastern Channel Islands Region, Southern California, *U.S. Geol. Surv. Open File Rep., 2005–1153*.

Davis, P. (2004), The marine terrace enigma of Catalina Island—An uplifting experience?, in *Geology and Tectonics of Santa Catalina Island and the California Continental Borderland*, *Field Trip Guidebook*, vol. 32, edited by M. Legg, P. Davis, and E. Gath, pp. 115–121, South Coast Geol. Soc., Santa Ana.

De Hoogh, G. L. (2012), Structural and stratigraphic evolution of the central and Southern Outer California Continental Borderland, unpublished MS thesis, California State Univ., Long Beach, 66 pp.

Dixon, T. H., et al. (2000), New kinematics for Pacific-North America motion from 3 Ma to present, II: Evidence for a Baja California shear zone, *Geophys. Res. Lett.*, *27*, 3961–3964, doi:10.1029/2000GL008529.

Dolan, J. F., and P. Mann (1998), *Active Strike-Slip and Collisional Tectonics of the Northern Caribbean Plate Boundary Zone*, *Geol. Soc. Am. Spec. Pap.*, *326*, 174.

Emery, K. O. (1958), Shallow submerged marine terraces of Southern California, *Geol. Soc. Am. Bull.*, *69*, 39–60.

Emery, K. O. (1960), *The Sea Off Southern California, A Modern Habitat of Petroleum*, 366 pp., John Wiley, New York.

Field, M. E., and W. C. Richmond (1980), Sedimentary and structural patterns on the northern Santa Rosa–Cortes Ridge, Southern California, *Mar. Geol.*, *34*, 79–98.

Fisher, M. A., V. E. Langenheim, C. Nicholson, H. F. Ryan, and R. W. Sliter (2009), Recent developments in understanding the tectonic evolution of the Southern California offshore area: Implications for earthquake-hazard analysis, in *The Southern California Continental Borderland*, *Geol. Soc. Am. Spec. Pap.*, vol. 454, edited by H. J. Lee and W. R., pp. 229–250, Earth Science in the Urban Ocean, Boulder, Colo.

Francis, R. D., and M. R. Legg (2010), Quaternary uplift and subsidence of Catalina Ridge and San Pedro Basin, Inner California Continental Borderland, offshore Southern California: Results of high-resolution seismic profiling, AGU, Fall Meeting 2010, Abstract T13C-2218.

Francis, R. D., M. R. Legg, and C. M. Castillo (2013), Basin and fault evolution in the Inner Borderland, offshore Southern California, Geol. Soc. Am., Annual Meeting, Denver, Colo.

Graymer, R. W., V. E. Langenheim, R. W. Simpson, R. C. Jachens, and D. A. Ponce (2007), Relatively simple through-going fault planes at large-earthquake depth may be concealed by the surface complexity of strike-slip faults, in *Tectonics of Strike-Slip Restraining and Releasing Bends in Continental and Oceanic Settings*, edited by W. D. Cunningham and P. Mann, *Geol. Soc. London Spec. Publ.*, *290*, 189–201.

Hanks, T. C., and W. H. Bakun (2002), A bilinear source-scaling model for **M**-log A observations of continental earthquakes, *Seismol. Soc. Am. Bull.*, *92*, 1841–1846.

Harding, T. P. (1985), Seismic characteristics and identification of negative flower structures, positive flower structures, and positive structural inversion, *AAPG Bull.*, *69*, 582–600.

Hauksson, E. (2011), Crustal geophysics and seismicity in Southern California, *Geophys. J. Int.*, *186*, 82–98, doi:10.1111/j.1365-246X.2011.05042.x.

Hauksson, E., and L. Jones (1988), The July 1986 Oceanside (M_L = 5.3) earthquake sequence in the Continental Borderland, Southern California, *Bull. Seismol. Soc. Am.*, *78*, 1885–1906.

Hauksson, E., W. Yang, and P. M. Shearer (2012), Waveform relocated earthquake catalog for Southern California (1981 to June 2011), *Bull. Seismol. Soc. Am.*, *102*(5), 2239–2244, doi:10.1785/0120120010.

Hauksson, E., H. Kanamori, J. Stock, M.-H. Cormier, and M. Legg (2013), Fracturing the eastern edge of the Pacific Ocean lithosphere as evidenced by seismicity in the abyssal plain off Baja California, Mexico, *Geophys. J. Int.*, doi:10.1093/gji/gg1467.

Helmberger, D. V., P. G. Sommerville, and E. Garnero (1992), The location and source parameters of the Lompoc, California earthquake of 4 November 1927, *Bull. Seismol. Soc. Am.*, *82*, 1678–1709.

Houseman, G. A., E. A. Neil, and M. D. Kohler (2000), Lithospheric instability beneath the Transverse Ranges of California, *J. Geophys. Res.*, *105*, 16,237–16,250, doi:10.1029/2000JB900118.

Howell, D. G., and J. G. Vedder (1981), Structural implications of stratigraphic discontinuities across the Southern California Borderland, in *The Geotectonic Development of California, Rubey*, vol. 1, edited by W. G. Ernst, pp. 535–558, Prentice Hall, Englewood Cliffs, N. J.

Humphreys, E. D., and B. H. Hager (1990), A kinematic model for the late Cenozoic development of Southern California crust and upper mantle, *J. Geophys. Res.*, *95*, 19,747–19,762, doi:10.1029/JB095iB12p19747.

Hutton, K., J. Woessner, and E. Hauksson (2010), Earthquake monitoring in Southern California for seventy-seven years (1932–2008), *Bull. Seismol. Soc. Am.*, *100*, 423–446.

InfoBank (2013), [Available at http://walrus.wr.usgs.gov/infobank/.]

James, T., G. Rogers, J. Cassidy, H. Dragert, R. Hyndman, L. Leonard, L. Nykolaishen, M. Riedel, M. Schmidt, and K. Wang (2013), Field studies target 2012 Haida Gwaii earthquake, *Eos Trans. AGU*, *94*(22), 197–198, doi:10.1002/2013EO220002.

Junger, A. (1976), Tectonics of the Southern California Borderland, in *Aspects of the Geological History of the California Continental Borderland*, *Pac. Sect., Misc. Publ. 24*, edited by D. G. Howell, pp. 486–498, Am. Assoc. Pet. Geol., Bakersfield, Calif.

Junger, A. (1979), Maps and seismic profiles showing geologic structure of the Northern Channel Islands Platform, California Continental Borderland, U.S. Geological Survey Miscellaneous Field Studies Map MF-991, Scale 1:250,000.

Junger, A., and H. D. Wagner (1977), Geology of the Santa Monica and San Pedro Basins, California Continental Borderland, U.S. Geological Survey, Miscellaneous Field Studies, Map MF-820, Scale 1:250,000.

Kamerling, M. A., and B. P. Luyendyk (1985), Paleomagnetism and Neogene tectonics of the northern Channel Islands, California, *J. Geophys. Res.*, *90*, 12,485–12,502, doi:10.1029/JB090iB14p12485.

Kamerling, M., and B. P. Luyendyk (1979), Tectonic rotations of the Santa Monica Mountains region, western Transverse Ranges, California, suggested by paleomagnetic vectors, *Geol. Soc. Am. Bull.*, *90*, 331–337.

Kennedy, M. P., and E. E. Welday (1980), Recency and character of faulting offshore Metropolitan San Diego, California. California Division of Mines & Geology, Map Sheet 40, Scale 1:50,000.

Kohler, M. D. (1999), Lithospheric deformation beneath the San Gabriel Mountains in the Southern California Transverse Ranges, *J. Geophys. Res.*, *104*, 15,025–15,041, doi:10.1029/1999JB900141.

Kohler, M. D., and The Science Party (2010), ALBACORE OBS deployment cruise report, R/V *Melville* Cruise MV1010, 27 pp., 14–27 Aug.

Lajoie, K. R., D. J. Ponti, C. L. Powell II, S. A. Mathieson, and A. M. Sarna-Wojcicki (1992), Emergent marine strandlines and associated sediments, coastal California; A record of Quaternary sea level fluctuations, vertical tectonic movements, climatic changes, and coastal processes, in *The Regressive Pleistocene Shoreline Coastal Southern California*, *Annual Field Trip Guide Book No. 20*, edited by E. G. Heath and W. L. Lewis, pp. 81–104, South Coast Geol. Soc., Santa Ana, Calif.

Lay, T., L. Ye, H. Kanamori, Y. Yamazaki, K. F. Cheung, K. Kwong, and K. D. Koper (2013), The October 28, 2012 M_w 7.8 Haida Gwaii underthrusting earthquake and tsunami: Slip partitioning along the Queen Charlotte Fault transpressional plate boundary, *Earth Planet. Sci. Lett.*, *375*, 57–70.
Legg, M. R. (1980), Seismicity and tectonics of the inner continental borderland of Southern California and northern Baja California, Mexico, unpublished MS thesis, Univ. of California, Santa Diego, Calif., 60 pp.
Legg, M. R. (1985), Geologic Structure and tectonics of the inner continental borderland offshore northern Baja California, Mexico, PhD dissertation, Univ. of California, Santa Barbara, Calif., 410 pp.
Legg, M. R. (1991), Developments in understanding the tectonic evolution of the California Continental Borderland, in *From Shoreline to Abyss*, vol. 46, edited by R. H. Osborne, pp. 291–312, SEPM Shepard Commemorative., Tulsa, Okla.
Legg, M. R., and R. D. Francis (2011), Submarine landslides at Santa Catalina Island, AGU, Annual Meeting, San Francisco, Calif., Abstract T33G-2507.
Legg, M. R., and C. Goldfinger (2002), Earthquake potential of major faults offshore Southern California, Collaborative research with Oregon State University and Legg Geophysical: U.S. Geological Survey Final Tech. Rep., Grant No. 01HQGR0017, 24 pp.
Legg, M. R., and M. J. Kamerling (2012), Basin inversion and the tectonic evolution of borderland strike-slip restraining bends, AAPG Annual Meeting, Long Beach, Calif., 25 April.
Legg, M. R., and M. P. Kennedy (1979), Faulting offshore San Diego and northern Baja California, in *Earthquakes and Other Perils: San Diego Region*, edited by P. L. Abbott and W. J. Elliott, pp. 29–46, San Diego Assoc. of Geol., San Diego, Calif.
Legg, M. R., B. P. Luyendyk, J. Mammerickx, C. de Moustier, and R. C. Tyce (1989), SeaBeam survey of an active strike-slip fault: The San Clemente fault in the California Continental Borderland, *J. Geophys. Res.*, *94*, 1727–1744, doi:10.1029/JB094iB02p01727.
Legg, M. R., V. Wong-Ortega, and F. Suarez-Vidal (1991), Geologic structure and tectonics of the Inner Continental Borderland of northern Baja California, in *The Gulf and Peninsular Province of the Californias*, *Mem.*, vol. 47, edited by J. P. Dauphin and B. R. T. Simoneit, pp. 145–177, Am. Assoc. Pet. Geol., Tulsa, Okla.
Legg, M. R., C. Nicholson, C. Goldfinger, R. Milstein, and M. Kamerling (2004), Large enigmatic crater structures offshore Southern California, *Geophys. J. Int.*, *158*, 803–815.
Legg, M. R., C. Goldfinger, M. J. Kamerling, J. D. Chaytor, and D. E. Einstein (2007), Morphology, structure and evolution of California Continental Borderland restraining bends, in *Tectonics of Strike-Slip Restraining and Releasing Bends in Continental and Oceanic Settings*, edited by W. D. Cunningham and P. Mann, *Geol. Soc. London Spec. Publ.*, *290*, 143–168.
Lonsdale, P. F. (1991), Structural patterns of the Pacific floor offshore of Peninsular California, in *The Gulf and Peninsular Province of the Californias*, *Mem.*, vol. 47, edited by J. P. Dauphin and B. R. T. Simoneit, pp. 87–125, Am. Assoc. Pet. Geol., Tulsa, Okla.
Luyendyk, B. P., P. B. Gans, and M. J. Kamerling (1998), $^{40}Ar/^{39}Ar$ Geochronology of Southern California Neogene volcanism, in *Contributions to the Geology of the Northern Channel Islands, Southern California*, edited by P. W. Weigand, pp. 9–47, Am. Assoc. Pet. Geol., Pacific Section, Ventura, Calif.
Magistrale, H. (1993), Seismicity of the Rose Canyon fault zone near San Diego, California, *Seismol. Soc. Am. Bull*, *83*, 1971–1978.
Magistrale, H., L. Jones, and H. Kanamori (1989), The Superstition Hills, California, earthquakes of 24 November 1987, *Seismol. Soc. Am. Bull*, *79*, 239–251.
Miller, K. C. (2002), Geophysical evidence for Miocene extension and mafic magmatic addition in the California Continental Borderland, *Geol. Soc. Am. Bull.*, *114*, 497–512.
Minster, J. B., and T. H. Jordan (1978), Present-day plate motions, *J. Geophys. Res.*, *83*, 5331–5354, doi:10.1029/JB083iB11p05331.
Moore, D. G. (1969), Reflection profiling studies of the California Continental Borderland structure and Quaternary turbidite basins, *Geol. Soc. Am. Spec. Pap.*, *107*, 142.
National Archive of Marine Seismic Surveys (NAMSS) (2006), [Available at http://walrus.wr.usgs.gov/NAMSS/.]
Nazareth, J. J., and E. Hauksson (2004), The seismogenic thickness of the Southern California crust, *Seismol. Soc. Am. Bull.*, *94*, 940–960.
Nicholson, C., and J. K. Crouch (1989), Neotectonic structures along the central and Southern California margin: Predominantly a thrust regime?, *Seismol. Res. Lett.*, *60*, 23–24.
Nicholson, C., C. C. Sorlien, and M. R. Legg (1993), Crustal imaging and extreme Miocene extension of the inner California Continental Borderland, *Geol. Soc. Am. Abstr. Programs*, *25*, 418.
Nicholson, C., C. C. Sorlien, T. Atwater, J. C. Crowell, and B. P. Luyendyk (1994), Microplate capture, rotation of the western Transverse Ranges, and initiation of the San Andreas transform as a low-angle fault system, *Geology*, *22*, 491–495.
Normark, W. R., S. Baher, and R. Sliter (2004), Late Quaternary sedimentation and deformation in Santa Monica and Catalina Basins, offshore Southern California, in *Geology and Tectonics of Santa Catalina Island and the California Continental Borderland*, *Annual Field Trip Guidebook*, edited by M. Legg, P. Davis, and E. Gath, pp. 291–317, South Coast Geol. Soc., Santa Ana, Calif.
Nur, A., and H. Ron (2003), Material and stress rotations: The key to reconciling crustal faulting complexity with rock mechanics, in *Thompson Volume: The Lithosphere of Western North America and its Geophysical Characterization*, *Geol. Soc. Am. Int. Book Ser.*, vol. 7, edited by S. L. Klemperer and W. G. Ernst, pp. 143–162, The George A, Boulder, Colo.
Plattner, C., R. Malservisi, T. H. Dixon, P. LaFemina, G. F. Sella, J. Fletcher, and F. Suarez-Vidal (2007), New constraints on relative motion between the Pacific plate and Baja California microplate (Mexico) from GPS measurements, *Geophys. J. Int.*, *170*, 1373–1380.
Rivero, C., J. H. Shaw, and K. Mueller (2000), Oceanside and Thirtymile Bank blind thrusts: Implications for earthquake hazards in coastal Southern California, *Geology*, *28*, 891–894.
Ryan, H. F., J. E. Conrad, C. K. Paull, and M. McGann (2012), Slip rate on the San Diego Trough fault zone, Inner California Borderland, and the 1986 Oceanside earthquake swarm revisited, *Seismol. Soc. Am. Bull*, *102*, 2300–2312.
Ryan, W. B. F., et al. (2009), Global Multi-Resolution Topography synthesis, *Geochem. Geophys. Geosyst.*, *10*, Q03014, doi:10.1029/2008GC002332.
Satake, K., and P. G. Sommerville (1992), Location and size of the 1927 Lompoc, California, earthquake from tsunami data, *Seismol. Soc. Am. Bull.*, *82*, 1710–1725.
Schindler, C. S. (2010), 3D fault geometry and basin evolution in the northern Continental Borderland offshore Southern California, unpublished MS thesis, California State Univ., Bakersfield, 42 pp.
Shepard, F. P., and K. O. Emery (1941), Submarine topography off the Southern California coast: Canyons and tectonic interpretation, *Geol. Soc. Am. Spec. Pap.*, *31*, 171.
Shintaku, N., D. S. Weeraratne, and M. D. Kohler (2010), Seafloor bathymetry and gravity from the ALBACORE marine seismic experiment offshore Southern California, Fall AGU, San Francisco, Calif., Abstract G43A-0831.
Slemmons, D. B. (1973), State-of-the-art for assessing earthquake hazards in the United States; Report 6: Faults and earthquake magnitude, Mackay School of Mines, U. Nevada, Reno, Vicksburg, U. S. Army Engineer Waterways Experiment Station, Misc. Pap. S-73-1, Rep. 6, Appendix A: Geomorphic features of active fault zones, p. 37.
Sorlien, C. (2002), Proposed objective for the SCEC Borderland Initiative Working Group, Southern California Earthquake Center (SCEC) Borderlands Initiative Workshop, March 8–10, 2002, Santa Catalina Island.

Sorlien, C. C., B. P. Luyendyk, L. Seeber, K. G. Broderick, W. R. Normark, M. A. Fisher, and R. W. Sliter (2013), The Palos Verdes anticlinorium along the Los Angeles, California coast: Implications for underlying thrust faulting, *Geochem. Geophys. Geosyst.*, *14*, 1866–1890, doi:10.1002/ggge.20112.

Spotila, J. A., M. A. House, N. A. Niemi, R. C. Brady, M. Oskin, and J. T. Buscher (2007), *Patterns of Bedrock Uplift Along the San Andreas Fault and Implications for Mechanisms of Transpression*, edited by A. B. Till et al., *Geol. Soc. Am. Spec. Pap.*, *434*, 15–33.

Sylvester, A. G. (1988), Strike-slip faults, *Geol. Soc. Am. Bull.*, *100*, 1666–1703.

Sylvester, A. G., and R. R. Smith (1976), Tectonic transpression and basement-controlled deformation in San Andreas fault zone, Salton Trough, California, *AAPG Bull.*, *60*, 2081–2102.

Tchalenko, J. S. (1970), Similarities between shear zones of different magnitudes, *Geol. Soc. Am. Bull.*, *81*, 1625–1640.

ten Brink, U. S., J. Zhang, T. M. Brocher, D. A. Okaya, K. D. Klitgord, and G. S. Fuis (2000), Geophysical evidence for the evolution of the California Inner Continental Borderland as a metamorphic core complex, *J. Geophys. Res.*, *105*, 5835–5857, doi:10.1029/1999JB900318.

Uchupi, E. (1961), Submarine geology of the Santa Rosa-Cortes Ridge, *J. Sediment. Petrol.*, *31*(4), 534–545.

Vedder, J. G. (1987), Regional geology and petroleum potential of the Southern California Borderland, in *Geology and Resource Potential of the Continental Margin of Western North America and Adjacent Ocean Basins—Beaufort Sea to Baja California: Earth Science Ser.*, vol. 6, edited by D. W. Scholl, A. Grantz, and J. G. Vedder, pp. 403–448, Circum-Pacific Council for Energy and Mineral Resources, Houston, Tex.

Vedder, J. G. (1990), Maps of California Continental Borderland showing compositions and ages of bottom samples acquired between 1968 and 1979, U.S. Geol. Surv. Misc. Field Stud. Map MF-2122, Scale 1:250,000.

Vedder, J. G., and M. I. Toth (1976), Proposed new geographic names for features in the California Continental Borderland, in *Aspects of the Geologic History of the California Continental Borderland, Pacific Section AAPG*, vol. 24, edited by D. G. Howell, pp. 12–14, Misc. Publ., Pacific Section, Bakersfield, Calif.

Vedder, J. G., L. A. Beyer, A. Junger, G. W. Moore, A. E. Roberts, J. C. Taylor, and H. C. Wagner (1974), Preliminary report on the geology of the Continental Borderland of Southern California, U.S. Geol. Surv. Misc. Field Stud. Map MF-624, Scale 1:500,000.

Vedder, J. G., D. G. Howell, and J. A. Forman (1979), Miocene strata and their relation to other rocks: Santa Catalina Island, California, in *Cenozoic Geology of the Western United States, Pacific Coast Paleogeography Symposium 3*, edited by J. M. Armentrout, M. R. Cole, and H. Terbest Jr., pp. 239–256, Soc. Econ. Paleontol. Mineral., Pacific Section, Los Angeles, Calif.

Vedder, J. G., H. G. Greene, S. H. Clarke, and M. P. Kennedy (1986), Geologic map of the mid-Southern California continental margin, California Division of Mines & Geology, California Continental Margin Geologic Map Series, Area 2 of 7, sheet 1 of 4, scale 1:250,000.

Weigand, P. W. (1994), Petrology and geochemistry of Miocene volcanic rocks from Santa Catalina and San Clemente Islands, California, in *Proceedings of the Fourth California Island Symposium*, edited by W. L. Halvorson and G. J. Maender, pp. 267–280, Santa Barbara Museum of Natural History, Santa Barbara, Calif.

White, B. C., M. R. Legg, and E. G. Frost (2004), Santa Catalina Island: A right-lateral restraining bend pop-up structure, in *Geology and Tectonics of Santa Catalina Island and the California Continental Borderland: Field Trip Guidebook No. 32*, edited by M. Legg, P. Davis, and E. Gath, pp. 123–140, South Coast Geol. Soc., Santa Ana, Calif.

Wilcox, R. E., T. P. Harding, and D. R. Seeley (1973), Basic wrench tectonics, *Am. Assoc. Pet. Geol. Bull.*, *57*, 74–96.

Wilson, D. S., P. A. McCrory, and R. G. Stanley (2005), Implications of volcanism in coastal California for the Neogene deformation history of western North America, *Tectonics*, *24*, TC3008, 1–22, doi:10.1029/2003TC001621.

Working Group on California Earthquake Probabilities (2003), Earthquake probabilities in the San Francisco Bay region: 2002–2031, *U.S. Geol. Surv. Open File Rep., 03–214*.

Wright, T. L. (1991), Structural geology and tectonic evolution of the Los Angeles Basin, in *Active Margin Basins*, *Mem.*, vol. 52, edited by K. T. Biddle, pp. 13–134, Am. Assoc. Pet. Geol., Tulsa, Okla.

Yang, W., E. Hauksson, and P. M. Shearer (2012), Computing a large refined catalog of focal mechanisms for Southern California (1981–2010): Temporal stability of the style of faulting, *Seismol. Soc. Am. Bull.*, *102*, 1179–1194.

Yeats, R. S., K. Sieh, and C. R. Allen (1997), *The Geology of Earthquakes*, *Tectonic Geomorphology*, chap. 7, pp. 139–164, Oxford Univ. Press, New York.